separations

MDPI

Review

Mechanism-Guided Deep Eutectic Solvents for Selective Metal Recovery from Solid Wastes: Linking Occurrence States to Closed-Loop Separation

Mingshi Wang, Enhui Xie, Aijun Lin, Leyun Wang * and Yong Xiao *

Department of Environmental Science and Engineering, Beijing University of Chemical Technology, Beijing 100029, China; 2025200209@buct.edu.cn (M.W.); 2025200214@buct.edu.cn (E.X.); linaj@buct.edu.cn (A.L.)
* Correspondence: lywang2025@buct.edu.cn (L.W.); xiaoyong@buct.edu.cn (Y.X.)

Abstract

Complex metal-containing solid wastes pose major recovery challenges because target metals and impurities coexist in different occurrence states and may be simultaneously transferred into deep eutectic solvent (DES) leachates. DESs offer tunable acidity, redox capacity, coordination environments, and solvation properties, enabling regulation of metal release and recovery. However, existing studies rarely integrate metal occurrence states, release barriers, liquid-phase speciation, phase partitioning, and downstream recovery. This Review develops a mechanism-guided framework linking solid-state characteristics with protonation, redox regulation, coordination stabilization, solvation, and mass transfer. Density functional theory, COSMO-RS, and machine learning are further integrated to elucidate molecular interactions, predict solvation and phase behavior, and identify multivariable relationships governing recovery performance. The framework extends from leaching to selective separation, product recovery, and DES regeneration. The analysis shows that high leaching efficiency alone does not ensure process viability, which also depends on selectivity, downstream recovery, solvent regeneration, and material and energy demands. By integrating these factors with environmental, economic, and engineering considerations, this Review provides a basis for designing selective, recyclable, and more sustainable DES-based metal recovery processes.

Keywords: deep eutectic solvents; solid waste metal recovery; metal occurrence states; release barriers; solvent design; closed-loop recovery

Check for updates

Academic Editor: Athanasia K. Tolkou

Received: 21 September 2026
Revised: 8 October 2026
Accepted: 13 October 2026
Published: 14 October 2026

Copyright: © 2026 by the authors. Licensee MDPI, Basel, Switzerland. This article is an open access article distributed under the terms and conditions of the Creative Commons Attribution (CC BY) license.

1. Introduction

Continued industrialization, the energy transition, and growing resource consumption are increasing both critical-metal demand and the generation of metal-containing solid wastes [1–3]. Spent batteries, spent catalysts, electronic waste, incineration fly ash, metallurgical slags, and mining wastes pose environmental risks but also contain substantial quantities of valuable metals [4–8]. Global electronic waste generation reached approximately 62 million tons in 2022 and is projected to reach 82 million tons by 2030. Although metal fractions accounted for approximately 31 million tons, only 22.3% was formally collected and recycled [3]. Metal recovery is therefore important for reducing environmental risks, strengthening resource supply security, and promoting the high-value utilization of solid wastes [2,9].

Metal recovery currently relies mainly on pyrometallurgical and aqueous hydrometallurgical processes. Pyrometallurgy can accommodate complex feedstocks but typically

requires temperatures above 1000 °C, resulting in high energy consumption and additional off-gas treatment and refining requirements [10,11]. Hydrometallurgy operates under milder conditions but often uses corrosive acids, bases, or redox reagents, which may cause impurity co-leaching and wastewater generation [12,13]. Emerging green recovery strategies increasingly seek to reduce energy and reagent consumption through alternative process routes and predictive process control. These include low-temperature physical-metallurgy approaches based on metallic affinity and phase partitioning, as well as data-driven models for predicting and optimizing metallurgical extraction processes [14,15]. Such developments highlight that greener metallurgy can be achieved through multiple technological pathways rather than through substitution of one extraction medium alone. Within this broader landscape, deep eutectic solvents (DESs) provide a complementary solvometallurgical approach because of their low volatility, relatively mild operating conditions, and compositional tunability [16–19]. Their acidity, redox capacity, and coordination environment can be tailored to promote the release of metals in different occurrence states [20–22].

DESs have been applied to spent batteries, spent catalysts, electronic waste, rare-earth permanent magnets, metallurgical residues, and mining wastes [23], with target-metal leaching efficiencies exceeding 90% in some systems [24,25]. However, the DES-based extraction process itself remains in pilot, scale-up, and pre-commercial development rather than mature full-scale industrial operation [26,27]. This gap reflects several interconnected challenges, including the high viscosity and mass-transfer limitations of many DESs, relatively high solvent-to-solid ratios, feedstock variability and impurity complexity, downstream separation requirements, solvent losses and composition changes during regeneration, and the associated energy and economic demands [23,28–31]. Consequently, high laboratory-scale leaching efficiency alone does not establish industrial viability.

The central challenge is therefore no longer simply to identify DES systems with high leaching efficiencies. Instead, it is necessary to understand why different waste-DES combinations produce different outcomes and use this knowledge to guide the future design of selective, recyclable, and scalable recovery systems. Different metal-binding modes impose distinct release barriers, whereas DESs provide different protonation, redox-regulation, and coordination-stabilization, solvation, and mass-transfer functions [20–22]. Conventional experiments provide macroscopic indicators such as leaching efficiency and selectivity but often cannot distinguish the specific contributions of bond cleavage, electron transfer, coordination stabilization, and multivariable coupling [32,33]. Computational and data-driven approaches are therefore needed to support mechanistic interpretation and enable the predictive design of DESs [33–35]. Moreover, process viability also depends on downstream separation, product recovery, DES regeneration, and environmental, economic, and engineering performance [28].

Existing reviews mainly discuss DES-based metal recovery according to waste type, solvent composition, or leaching performance [28,36]. The relationships among metal occurrence states, release barriers, DES functions, predictive design, and downstream processing remain insufficiently addressed. Protonation, redox regulation, and coordination stabilization are also commonly discussed separately, although these processes are coupled in actual leaching systems [31]. Table 1 compares representative reviews and highlights the limited integration of metal occurrence states, release mechanisms, predictive design, and downstream recovery.

Table 1. Comparison of the scope, organization, and emphasis of representative reviews on DES-based metal recovery.

Representative Review	Research Scope and Organization	Coverage Relative to the Present Framework
[37]	Focuses on spent lithium-ion battery cathode materials and is organized around the recycling process and DES properties	Mainly limited to spent LIBs, with relatively little coverage of other solid wastes
[38]	Covers various metal-containing wastes, with emphasis on DES physicochemical properties and application areas	Primarily summarizes DES properties and applications, with limited discussion of solid-state metal forms and process interconnections
[39]	Focuses on critical raw materials from spent LIBs and is organized around hydrometallurgical recovery and IL/DES-based separation technologies	Covers both ILs and DESs and mainly focuses on spent LIBs
[36]	Focuses on spent LIBs and is organized according to recycling stages and DES types	Mainly focuses on spent LIB recycling, with limited coverage of other solid-waste systems
[29]	Covers multiple metal-containing solid wastes and is organized by waste type, DES system, and leaching performance	Systematically summarizes waste types, DES systems, and leaching performance, but provides limited mechanistic analysis and multiscale design discussion
[30]	Covers various metal resources and environmental matrices and is organized by metal source, extraction mechanism, and separation method	Covers a broad range of topics, but provides limited integration across process stages and limited discussion of rational DES design
[23]	Covers various secondary resources and is organized by resource type, DES performance, and selective recovery	Broad in scope, but provides limited integration among mechanisms, solvent properties, and whole-process performance
[40]	Covers primary minerals and various secondary resources from a mineral-processing and engineering-process perspective	Provides systematic discussion of recycling and engineering issues, but gives limited attention to mechanistic analysis and computationally assisted design

This review takes metal occurrence states and their associated release barriers as its starting point and links them to specific DES-assisted mechanisms [41]. It further examines how density functional theory (DFT), conductor-like screening model for real solvents (COSMO-RS), and machine learning (ML) can translate experimental observations into interpretable and predictive criteria for solvent design [33–35], while extending the analysis to separation, product recovery, DES regeneration, and process feasibility [23]. Specifically, the proposed framework guides the prioritization of DES functions, the selection of appropriate diagnostic characterization, and the identification of key process limitations for different release barriers.

The literature included in this Review was identified through searches of Web of Science, Scopus, and ScienceDirect, covering publications available up to September 2026. Search terms included combinations of "deep eutectic solvent" or "DES" with "metal leaching", "metal recovery", "selective separation", "solvent regeneration", "spent lithium-ion batteries", "spent catalysts", "electronic waste", "metallurgical residues", "mining wastes", and related terms. Studies were included when they reported DES-based or DES-assisted metal recovery and provided relevant information on metal occurrence states, leaching mechanisms, separation, product recovery, solvent regeneration, or quantitative process performance. Studies were excluded when they were unrelated to metal recovery,

lacked sufficient methodological or quantitative information, or duplicated data reported elsewhere. Representative studies were further selected to ensure diversity in waste types, DES functions, and mechanistic evidence.

2. Influence of Metal Occurrence States in Solid Wastes on Leaching

Metal recovery from solid wastes is governed not only by total metal content but also by the occurrence states of target metals within the solid matrix [42–44]. Depending on waste origin, initial material composition, and subsequent environmental transformation, metals may occur in several distinct forms. These include water-soluble or exchangeable species, surface-adsorbed species, discrete mineral phases, lattice- or matrix-bound species, and metallic or alloy phases [42]. These occurrence states define the local bonding environments of target metals and shape the dominant barriers to their transfer from the solid into the liquid phase [45–47]. Metal release can involve interfacial desorption, phase dissolution, chemical-bond cleavage, lattice restructuring, or valence-state conversion [43]. Speciation and mineralogical characteristics can therefore identify the dominant release barriers and guide the prioritization of DES functions. Relevant functions include proton activation, redox regulation, coordination stabilization, solvation, and mass-transfer enhancement.

2.1. Interfacial Desorption- and Exchange-Controlled Release

Metals located on particle surfaces, within pore channels, at mineral edges, or at exchangeable sites are generally held by relatively weak electrostatic, ion-exchange, or local coordination interactions [48]. Their release is therefore governed primarily by interfacial desorption, ion exchange, and pore-scale mass transfer. Cd in municipal solid-waste-incineration fly ash provides a representative example. Sequential extraction shows that Cd is concentrated mainly in water-soluble and exchangeable fractions, indicating high release potential under suitable chemical conditions [49]. Van Herck and Vandecasteele [44] further related sequential-extraction results to leaching behavior at different endpoint pH values. Their analysis showed that speciation and mineralogical information can identify the chemical conditions required for metal release. For weakly bound metals, DES design can therefore prioritize interfacial exchange, solvation, and stabilization of released species while maintaining selectivity over matrix components.

2.2. Phase and Structure-Controlled Release

When target metals occur as discrete oxides, sulfides, phosphates, or composite mineral phases, their release is jointly governed by phase stability, solubility, initial oxidation state, and dissolved-species stability [23]. In spent Co-Mo hydrodesulfurization catalysts, Mo can be distributed across both oxide- and sulfide-containing phases [50]. Relative to acid treatment alone, adding an oxidizing agent markedly enhances Mo dissolution [50]. This response suggests that sulfides and elemental sulfur act as important redox-sensitive release barriers. When discrete-phase stability dominates metal release, DES design can target phase transformation, valence-state regulation, and stabilization of dissolved species. Such systems require functional matching, in which protonation, redox, and coordination functions are selected according to the chemical characteristics of the target phase. This strategy replaces the indiscriminate strengthening of a single solvent property with targeted control of the relevant release barrier.

Metals incorporated into host lattices, layered structures, or aluminosilicate frameworks experience stronger structural constraints. Their release often requires changes in the local coordination environment, weakening of metal-oxygen bonds, and, in some systems, partial restructuring of the host framework [51]. Layered NCM materials provide a representative example. During two-stage leaching, formic acid preferentially releases Li, while

Ni, Co, and Mn remain largely within the transition-metal framework [52]. This selective behavior reflects the greater accessibility of Li and the stronger local bonding constraints within the transition-metal sublattice. For lattice or framework-bound metals, DES design requires coordinated control of proton activation, M-O bond weakening, dissolved-species stabilization, and mass-transfer enhancement. Integrating these functions can preserve differentiated responses between target metals and structural matrix elements.

2.3. Redox-Controlled Release of Metallic and Alloy Phases

Metallic and alloy phases follow a distinct release pathway in which dissolution is initiated by valence-state conversion. Zero-valent Pt, Pd, Rh, and Au generally require oxidation before ligands such as halides can stabilize them as ionic or complexed species [53–55]. In spent automotive catalysts, sintering, support transformation, and surface deposits can further influence the accessibility and oxidation behavior of metal particles [56]. In spent Pd/Al_2O_3 catalysts, the combined presence of Fe^{3+} and sufficient Cl^- markedly enhances Pd dissolution [57]. This response identifies metallic-Pd oxidation followed by ligand stabilization in the liquid phase as a key release pathway. DES design for metallic or alloy-bound elements can therefore couple redox activation with complex stabilization to sustain metal transfer from the solid phase into solution.

Overall, metal occurrence states determine the dominant release barriers encountered during leaching, and these barriers provide a direct basis for prioritizing DES functions [58]. Weakly bound metals are governed mainly by desorption and exchange, whereas discrete mineral phases respond more strongly to phase stability and valence-state transformation. Lattice or framework-bound metals are controlled by local bonding and structural constraints. Metallic or alloy-bound elements generally require valence-state conversion followed by complex stabilization. Table 2 translates the occurrence-state framework into a practical decision matrix by linking dominant release barriers with the DES functions that should be prioritized, the characterization methods that can support barrier identification, and the major limitations that may arise during leaching. The matrix is intended as a decision-support framework rather than a one-to-one classification, because multiple release barriers and mechanisms may coexist in complex waste matrices and their relative contributions depend on the specific barrier controlling metal release. Within this framework, DES design can move beyond acidity maximization toward targeted matching of solvent functions to the specific solid-state environment. These functions include proton activation, redox capacity, coordination strength, solvation behavior, and mass-transfer properties [30]. This barrier-oriented strategy promotes target-metal release while supporting selectivity, dissolved-species stabilization, and reduced downstream separation requirements.

Table 2. Practical decision matrix linking metal occurrence states with release barriers, required DES functions, diagnostic characterization, and key limitations.

Occurrence State Category	Solid Waste Type	Metal	Main Release Barrier	Required DES Function	Diagnostic Characterization	Key Limitation	References
Weakly bound state	MSWI fly ash	Cd	Interfacial desorption and ion exchange	Solvation, interfacial exchange	Sequential extraction, pH-dependent leaching	Co-extraction of weakly bound species	[44,49]
Discrete-phase-bound state	Spent Co-Mo hydrodesulfurization catalyst	Mo	Mo–S bond cleavage and oxidation of sulfide phases	Protonation, redox regulation, coordination	XRD, XPS	Impurity co-leaching	[50]
Discrete-phase- and support-associated state	Spent Ni-Mo/γ-Al_2O_3 catalyst	Mo	Disruption of MoS_2/NiMoS structures and metal–support interactions	Protonation, redox regulation, coordination	XRD, XPS, SEM–EDS	High reagent demand and support co-dissolution	[59,60]
		Ni	Disruption of Ni–Mo–S structures and Ni–S bonding; metal–support interactions	Protonation, redox regulation, coordination	XRD, XPS, SEM–EDS	Incomplete release and support co-dissolution	[59,61]
Lattice-or matrix-bound state	Layered NCM cathode material	Li	Li–O bonding and structural constraints on interlayer deintercalation	Proton activation, solvation	XRD, XPS	Limited release under insufficient proton activation	[52,62,63]
	Layered NCM cathode material	Ni	Ni–O bond weakening and local MO_6 framework disruption	Protonation, redox regulation, coordination	XRD, XPS, XANES/EXAFS	Slow lattice disruption	[22,63]
		Co	Co–O bond cleavage and lattice disruption, coupled with valence-state regulation	Protonation, reduction, coordination	XRD, XPS, XANES/EXAFS	Reductant demand and co-leaching	[21,22]
		Mn	Mn–O bond cleavage, valence constraints, and lattice disruption	Protonation, redox regulation, coordination	XRD, XPS, XANES/EXAFS	Redox dependence and co-leaching	[22,63]
Lattice-/framework-bound and mineral-associated state	Coal gangue	REYs (including Y, La, and Ce)	Aluminosilicate-framework disruption and dissolution of REE-bearing mineral phases	Proton activation, coordination, solvation	XRD, SEM–EDS, sequential extraction	Matrix dissolution and high reagent demand	[64,65]
Metallic or alloy state	Spent Pd/Al_2O_3 catalyst	Pd	Oxidation of Pd^0 and limited accessibility of reactive sites	Oxidative activation and complexation	XPS, XANES/electrochemical analysis	Oxidant consumption and mass-transfer limitation	[56,57]

3. Mechanisms Governing DES-Assisted Targeted Metal Leaching

DESs have been applied to spent lithium-ion batteries, industrial spent catalysts, rare-earth permanent magnets, metallurgical residues, and mining wastes [23]. However, their leaching performance varies widely across feedstocks and DES formulations. Table 3 summarizes representative DES systems and their performance in recovering metals from different solid wastes. In this review, leaching efficiency refers to the fraction of a metal transferred from the initial solid feed into the leaching phase, selectivity describes the preferential leaching or separation of the target metal relative to coexisting species, and overall recovery refers to the fraction of the initial target metal ultimately recovered as an isolated product. The compiled data show that REE leaching efficiencies from some mine tailings remain below 25% [66]. By contrast, transition-metal leaching efficiencies in certain battery and catalyst systems approach 100% [24,25]. These differences cannot be attributed solely to solvent acidity or operating severity. Metal transfer from the solid to the liquid phase is instead governed by three coupled functions. Protonation initiates interfacial dissolution, redox regulation changes metal valence states, and coordination stabilizes released species or selectively removes them from solution. The contribution of each function depends on the metal occurrence states and initial release barriers discussed in Section 2 [67].

Mechanistic interpretations are distinguished by evidence level. Directly supported mechanisms are based on spectroscopic, structural, or electrochemical evidence, with computational results providing complementary mechanistic support. Interpretations derived mainly from leaching trends are treated as inferred, and cross-study comparisons are used to identify trends rather than establish direct causality.

Table 3. Representative applications of DESs for metal leaching from different solid wastes: operating conditions and leaching performance.

Solid Waste Category	Solid Waste Type	Target Metal(s)	DES Composition	Component Ratio (Water Content)	Temperature	Time	Liquid-to-Solid Ratio	Leaching Efficiency	Reference
Spent lithium-ion batteries	Commercial/model $LiCoO_2$ powder	Li, Co	ChCl-EG	1:2	220 °C	24 h	50 $g \cdot g^{-1}$	Li 89.8%; Co 94.1%	[22]
	Simulated $LiCoO_2$-Al-Cu cathode mixture	Li, Co (Cu, Al)	ChCl-CA + H_2O	2:1 35 wt.% H_2O	40 °C	60 min	50 $mL \cdot g^{-1}$	Co 98%; Li 93%; Cu 94%; Al 38%	[21]
	Spent LIB cathode material	Li (Co, Ni, Mn)	ChCl-U-EG	1:2:1	100 °C	72 h	9.69 $mL \cdot g^{-1}$	Li 92.83%; Co 1.61%; Ni 0.72%; Mn 0.42%	[62]
	Spent LCO cathode material	Li, Co, Ni, Mn	GuHCl-LA + AA	1:2 1 wt.% ascorbic acid	50 °C	24 h	50 $mL \cdot g^{-1}$	LCO: Li 97.42%; Co 96.91%	[68]
	Spent NCM cathode material	Li, Ni, Co, Mn	TEAC-L-AA	1:1	80 °C	3 min	40 $mL \cdot g^{-1}$	Li 99.1%; Ni 99.6%; Co 99.4%; Mn 99.3%	[24]
	Spent LNCM111 cathode powder	Li, Ni, Co, Mn	VC-DMSP chloride- H_2O	1:2	50 °C	14 min	40 $mL \cdot g^{-1}$	Li 99.92%; Co 99.84%; Mn 99.27%; Ni 99.67%	[69]
	Spent NCM cathode material	Li, Mn (Co, Ni)	EG-EtOH-CA	6:6:1	150 °C	16 h	125 $mL \cdot g^{-1}$	Li 94.4%; Mn 52.6%; Co, Ni < 15%	[70]
	Spent NCM622 cathode material	Li, Ni, Co, Mn	TEAC-PA	1:4	90 °C	60 min	50 $g \cdot g^{-1}$	Li 99.66%; Ni 99.13%; Co 99.08%; Mn 99.38%	[41]
	Spent NCM cathode active material	Li, Ni, Co, Mn	ChCl-PPA	1:2	100 °C	80 min	90 $mL \cdot g^{-1}$	Li 97.7%; Co 97.0%; Ni 96.4%; Mn 93.0%	[71]
	Spent $LiCoO_2$ cathode active material	Li, Co	ChCl-OA- H_2O	1:1:1	100 °C	2 h	66.7 $mL \cdot g^{-1}$	Li 99.99%; Co 99.99%	[72]
	$LiCoO_2$ cathode material	Li, Co	hydrated ChCl-CA	1:1 25.7 wt.% H_2O	120 °C	4 h	50 $mL \cdot g^{-1}$	Li 100%; Co 97.6%	[73]

Table 3. *Cont.*

Solid Waste Category	Solid Waste Type	Target Metal(s)	DES Composition	Component Ratio (Water Content)	Temperature	Time	Liquid-to-Solid Ratio	Leaching Efficiency	Reference
Spent industrial catalysts	Spent heavy-oil hydrotreating catalyst	V, Mo (Ni)	ChCl-OA + H_2O	1:2 H_2O/DES = 0.3 v/v	80 °C	3 h	20 mL·g^{-1}	V 97.8%; Mo 95.1%; Ni 1.8%	[74]
	Spent Ni-Mo hydrodesulfurization catalyst	Mo, Ni, Al, P	ChCl-PTSA	1:1	120 °C	8 h	200 mL·g^{-1}	Mo 98%; Ni 100%; Al 98%; P 100%	[25]
	Spent hydrodesulfurization catalyst	Ni, Mo, V (Al)	BeCl-PTSA + H_2O	1:2 45 wt.% H_2O	90 °C	180 min	100 mL·g^{-1}	Ni 90.03%; Mo 98.60%; V 94.98%; Al 9.82%	[75]
	Steam methane reforming catalyst and pyrolysis-gasoline hydrogenation catalyst	Ni	ChCl-PTSA-EG	1:2:1	100 °C	48 h	50 mL·g^{-1}	Ni > 90%	[76]
Rare-earth permanent magnet waste	Spent NdFeB permanent magnet	Nd (Fe)	GuHCl-LA	1:2	70 °C	5 h	100 g·g^{-1}	Nd > 96%; Fe 96.7%	[77]
	Spent NdFeB permanent magnet	Nd (Fe)	EG-MaleA	4:1	70 °C	5 h	100 g·g^{-1}	Nd 97.3%; Fe 0.84%	[77]
Non-ferrous metallurgical waste	Copper converter slag	Cu, Zn (Fe)	ChCl-U	1:2	95 °C	48 h	20 mL·g^{-1}	Cu 89.9%; Zn 65.3%; Fe $\leq$ 4.7%	[78]
	Zinc oxide dust	Zn	ChCl-U-EG	2:4:1	80 °C	48 h	20 mL·g^{-1}	Zn 85.2%	[79]
	Zinc oxide dust	Zn	ChCl-U + NTA	1:2 NTA 0.07 mol L^{-1}	79.0 °C	35.4 h	12.1 mL·g^{-1}	Zn 87.9%	[80]
	Zinc-industry goethite residue	Zn (Fe)	LevA-ChCl + H_2O	2:1 30 wt.% H_2O	30 °C	24 h	10 mL·g^{-1}	Zn 37%; Zn/Fe = 4.3	[81]
	Zinc-industry goethite residue	Zn (Fe)	LevA-ChCl + H_2O	2:1 30 wt.% H_2O	60 °C	24 h	10 mL·g^{-1}	Zn 65%; Zn/Fe = 0.8	[81]

Table 3. *Cont.*

Solid Waste Category	Solid Waste Type	Target Metal(s)	DES Composition	Component Ratio (Water Content)	Temperature	Time	Liquid-to-Solid Ratio	Leaching Efficiency	Reference
Coal-derived and mining wastes	Fe-rich mine tailings	TREE (Fe)	ChCl-PTSA	2:1	80 °C	96 h	NR	TREE 95%; Fe 95%	[82]
	Lovozero mine tailings	REEs, Zr, Nb, Hf, Ta	ChCl-CA + H_2O	1:1 30 wt.% H_2O	25 °C	14 d	10 $g \cdot g^{-1}$	REEs: 10.2–24.4%; Zr 8.2%; Nb 12.4%; Hf 8.3%; Ta 6.0%	[66]
	Coal-series kaolin	REEs (Al, Fe, Si)	BeCl-DL-MA + H_2O	1:3 30 wt.% H_2O	100 °C	180 min	30 $g \cdot g^{-1}$	REEs: 80.28–84.94%; Al 87.09%; Fe 75.59%; Si 10.47%	[64]

AA, ascorbic acid; BeCl, betaine hydrochloride; CA, citric acid; ChCl, choline chloride; DL-MA, DL-malic acid; DMSP, dimethyl-β-propiothetin chloride; EG, ethylene glycol; EtOH, ethanol; GuHCl, guanidine hydrochloride; LA, lactic acid; L-AA, L-ascorbic acid; LCO, lithium cobalt oxide; LevA, levulinic acid; LIB, lithium-ion battery; LNCM111, $LiNi_{1/3}Co_{1/3}Mn_{1/3}O_2$; MaleA, maleic acid; NCM, nickel–cobalt–manganese; NTA, nitrilotriacetic acid; OA, oxalic acid; PA, pyruvic acid; PPA, phenylphosphinic acid; PTSA, p-toluenesulfonic acid; REEs, rare-earth elements; TEAC, tetraethylammonium chloride; TREE, total rare-earth elements; U, urea; VC, vitamin C (ascorbic acid). NR, not reported.

3.1. Acid Dissolution and Protonation

Acid dissolution and protonation provide the initial driving force for metal release by activating solid surfaces and weakening metal-oxygen or metal-framework bonds [20]. In the ChCl-U-EG system, Li is released much more readily than Co, Ni, and Mn. This contrast is consistent with different initial release barriers for interlayer Li and transition metals embedded within the metal–oxygen framework [62]. The extent to which protonation promotes leaching therefore depends strongly on the specific barrier associated with the target metal.

Depending on the proton source, acidity in DES systems may be intrinsic or externally introduced. Intrinsic acidity arises from dissociable protons supplied by DES components, typically those containing carboxylic, sulfonic, or phosphoric acid groups [83–86]. External acidity is introduced through added inorganic or organic acids and provides a more direct increase in proton availability [87]. However, it may also intensify the co-leaching of support and impurity elements [87]. In intrinsically acidic DESs, leaching is governed mainly by the acidic structure of the components and their intermolecular interactions. Increasing the proportion of the acidic component in a ChCl-PTSA system enhanced Mo, Ni, and Al leaching from spent hydrodesulfurization catalysts [25]. Likewise, replacing the weakly acidic EG in ChCl-EG with a more acidic carboxylic-acid hydrogen-bond donor markedly promoted Co dissolution from $LiCoO_2$ [21]. These observations suggest that acidic functional groups facilitate metal release by enhancing protonation and weakening M-O bonds.

When the protons supplied by DES components are insufficient to disrupt stable mineral phases or crystal lattices, additional acid may be required in weakly acidic DES systems. In weakly acidic DESs, external acids may determine whether a metal can be effectively released rather than simply increasing its leaching efficiency. For example, adding 0.8 M HCl to ChCl-EG increased Co leaching from $LiCoO_2$ from approximately 5% to nearly 100% [87]. Comparable enhancement has been reported for HCl-assisted DES systems, strong acid-driven dissolution has also been observed in a conventional aqueous H_2SO_4 system [87,88]. Greater acidity may, however, also promote dissolution of Al_2O_3 supports and other impurities, thereby reducing selectivity [88]. Organic acids behave differently because their conjugate bases can regulate metal speciation or form sparingly soluble salts [89]. In a ChCl-oxalic acid-H_2O system for spent heavy-oil hydrotreating catalysts, V and Mo were preferentially leached [74]. Meanwhile, Ni remained in the solid phase as nickel oxalate, and the Al_2O_3 support remained largely stable [74]. Compared with the broad dissolution induced by strong inorganic acids, organic-acid-based DESs can more effectively couple protonation with coordination and selective precipitation. This coupling provides greater control over reaction pathways and metal-species distribution.

Acidity should therefore not be optimized as an isolated concentration parameter but considered within the broader functional combination of the DES [90,91]. For weakly bound or interlayer metals, intrinsic acidity may be sufficient to promote release while limiting matrix dissolution. Stable lattices and mineral phases often require external acid addition. In such cases, bond-cleavage ability must be balanced against metal-species regulation and impurity co-leaching. Limited improvement with increasing proton availability may indicate constraints imposed by lattice stability, dissolved-species coordination, or interfacial mass transfer [90,91]. DES acidity should therefore be evaluated together with water content, viscosity, and metal-ligand interactions.

3.2. Redox Regulation

When metal release requires a change in oxidation state, protonation alone is often insufficient for efficient leaching [92,93]. High-valent transition-metal oxides generally re-

quire reduction to facilitate M-O bond cleavage [92]. By contrast, zero-valent metals, alloys, and some sulfides must be oxidized before entering the liquid phase [93]. Redox regulation can therefore be classified as reductive dissolution or oxidative activation according to the electron-transfer direction required by the target phase.

Reduction is often critical for overcoming lattice stability and promoting the release of high-valent transition metals. This requirement is particularly evident in layered battery cathodes. Acidity alone tends to release Li, whereas Co, Ni, and Mn remain constrained by strong M-O bonds and high oxidation states. In a ChCl-U-EG system without appreciable reducing ability, Li was preferentially leached, while Co, Ni, and Mn leaching efficiencies remained below 2% [62]. Introducing L-ascorbic acid increased the leaching efficiencies of all three transition metals to above 99% [24,69] (Figure 1). Although the feedstocks and operating conditions were not completely identical, the overall trend is consistent with an important role of reducing components in promoting transition-metal release. These findings support an important role of reductive electron transfer in promoting transition-metal release. Electron donation lowers metal oxidation states, weakens M–O bonds, and enables otherwise inaccessible high-valent metals to enter the liquid phase. Zero-valent metals, alloys, and some sulfides instead require oxidative activation before effective dissolution. Oxidizing agents or redox-active species can promote metal oxidation and facilitate subsequent complexation and transfer into the liquid phase [55,94,95]. This effect is also reflected in I_2 assisted DES systems, where Au leaching can exceed 60% [53]. Following oxidation, Cl^-, Br^-, or I^- stabilizes the resulting metal species as halide complexes [96]. This stabilization promotes continued transfer into the liquid phase and suppresses redeposition. Nevertheless, stronger oxidative conditions cannot universally overcome structural limitations within the solid phase. Under comparable oxidative DES conditions, chalcopyrite conversion can exceed 95%, whereas structurally more stable pyrite shows only approximately 5% conversion [53]. Redox regulation therefore promotes metal release by converting stable occurrence forms into oxidation states that can be more readily dissolved and stabilized through coordination. The required electron-transfer direction depends on the initial oxidation state and occurrence form of the metal. Practical applications must also consider impurity co-leaching, reagent consumption, and DES cycling stability to avoid transferring environmental burdens downstream [31,97,98].

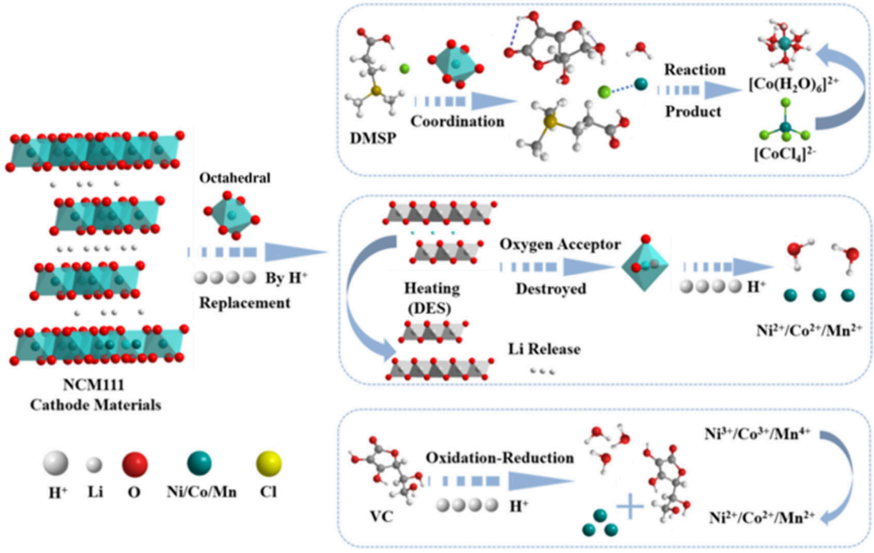


Figure 1. Coupled protonation, redox regulation, and coordination mechanisms during the DES-assisted leaching of lattice-bound transition metals from NCM111 cathode materials. Adapted from Ref. [69] with permission from the Royal Society of Chemistry, Copyright 2025.

3.3. Complexation and Coordination Stabilization

Metal release from the solid phase does not by itself complete the leaching process. Effective recovery requires dissolved metal species to remain stable in the liquid phase. Water addition and subsequent processing may induce hydrolysis, reprecipitation, or surface readsorption, returning dissolved metals to the solid phase [68]. This limitation is illustrated by lactic-acid-based rare-earth systems, in which dissolution depends strongly on the initial REE phase and on the stability and solubility of REE–lactate complexes; under the tested conditions, the DES showed no clear advantage over aqueous lactic acid [99]. Based on the final fate of coordinated metal species, coordination effects can be divided into three modes [100]. Soluble complexes stabilize target metals, charged complexes undergo ion association and interphase transfer, and sparingly soluble species retain selected metals in the solid phase.

Soluble-complex formation is the most common stabilization pathway, although ligand preferences differ among metals. Co^{2+} generally occurs predominantly as $[CoCl_4]^{2-}$ in ChCl-based DESs [101]. By contrast, Ni^{2+} can shift between chloride-coordinated and mixed Cl^-/HBD-coordinated structures depending on the properties of the HBD [101]. Mo and V are more readily stabilized as oxygen-containing or oxychloride species [75,102]. Nd^{3+}, Y^{3+}, and other rare-earth ions generally exhibit stronger affinities for carboxylate and phosphorus-containing O-donor ligands [103–105]. Appropriate metal-ligand interactions can substantially broaden the range of metals maintained in solution. They can also raise target-metal leaching efficiencies from low levels to above 90% [75,105]. These findings support an important role of coordination stabilization in sustaining metal transfer into the liquid phase.

For metals capable of forming charged complexes, coordination can couple with ion exchange or association to control interphase distribution. After oxidation and release, Pd can form $[PdCl_4]^{2-}$ in chloride-rich media. In quaternary-ammonium-based hydrophobic DESs, this anionic complex can replace Cl^- and form ion pairs with quaternary ammonium cations. This interaction enables selective transfer of Pd into the DES phase. Under optimized conditions, the single-stage Pd extraction efficiency exceeds 99% [106]. The phase distribution of precious metals is therefore governed jointly by halide-complex formation and ionic association with charged DES components.

Coordination can also generate selectivity by forming sparingly soluble species that suppress metal transfer into the liquid phase [107]. Carboxylate ligands are particularly effective in altering the dissolution states of different metals. Citrate forms soluble Co-O complexes with Co^{2+}, whereas oxalate precipitates Ni^{2+} as insoluble $NiC_2O_4{\cdot}2H_2O$ [74,107]. This difference has been exploited for the selective leaching of spent catalysts. In a ChCl-oxalic acid-H_2O system, V and Mo leaching efficiencies reached 97.8% and 95.1%, respectively, whereas Ni leaching was only 1.8% [74]. Coordination can therefore promote metal transfer through soluble-complex formation or suppress co-leaching through selective precipitation.

The significance of coordination is thus not limited to increasing metal solubility. Rather, coordination controls the ultimate fate of released metals [108]. Table 4 should therefore be interpreted as a correspondence between ligand type and process function, rather than simply as a catalog of coordination complexes. In practical DES systems, coordination does not occur independently. It is coupled with protonation, redox reactions, water content, viscosity, and competitive complexation among multiple metals [38]. A ligand that strongly stabilizes the target metal may also stabilize impurities [109]. Strong complexation may also complicate downstream product precipitation and solvent regeneration [110]. These mechanisms should not be interpreted as having a one-to-one correspondence with specific metal occurrence states, because multiple mechanisms may operate simultaneously

and their relative contributions depend on the dominant release barriers. The relationships among metal occurrence states, release barriers, and the major DES-assisted leaching mechanisms are summarized in Figure 2.

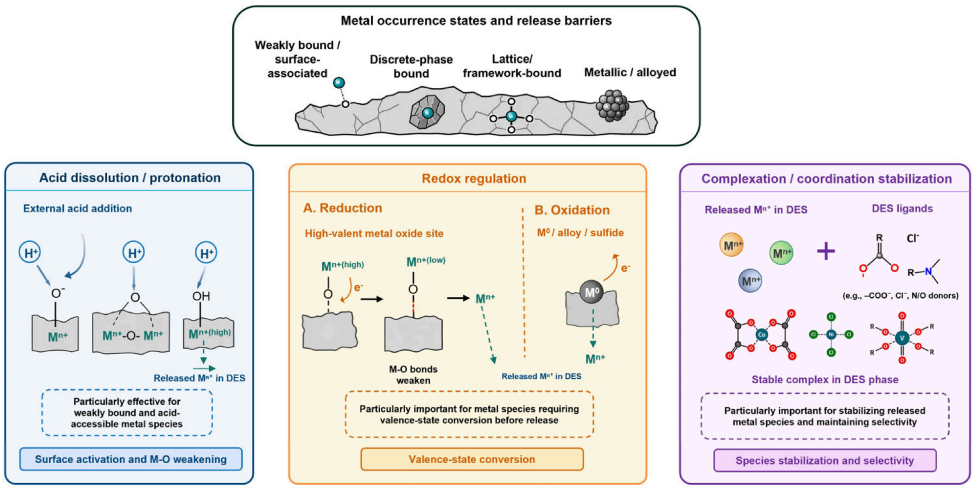


Figure 2. Metal occurrence states, release barriers, and coupled mechanisms of DES-assisted leaching.

Table 4. Representative metal–ligand coordination modes in DESs and their effects on metal leaching, speciation, and separation.

Metal Species	Major Ligand/ Coordinating Group	Representative DES System	Major Coordination/ Speciation Behavior	Effect on Leaching, Speciation, or Separation	References
Co^{2+}	Halide ligands	ChCl–EG	Formation of $[CoCl_4]^{2-}$	Stabilizes dissolved Co species	[101]
	Carboxylate O–donors	ChCl–CA	Formation of Co–O coordination species	Enhances Co liquid–phase stability	[21]
Ni^{2+}	Halide ligands	ChCl–EG	Formation of predominantly chloride–coordinated Ni species with EG participation	Stabilizes dissolved Ni species	[101]
	Carboxylate O–donors	ChCl–OA	Formation of $NiC_2O_4{\cdot}2H_2O$	Suppresses Ni co–leaching	[74]
	P–O donor ligands	ChCl–PPA	Formation of $P{=}O^-$ coordinated Ni species	Stabilizes dissolved Ni species	[71]
V(IV)	Halide ligands	BeCl–PTSA	Formation of chloro/oxychloro V species	Stabilizes dissolved V species	[75]
Mo(VI)	Halide ligands	BeCl–PTSA	Formation of chloro/oxychloro Mo species	Stabilizes dissolved Mo species	[75]
	Carboxylate O–donors	ChCl–OA	Oxalate–associated Mo coordination	Promotes Mo dissolution	[74]
Pd^{2+}	Halide ligands	$[N_{8881}]Cl$–1–hexanol	Association of $[PdCl_4]^{2-}$ with $[N_{8881}]^+$	Enhances Pd extraction	[106]
REE^{3+}	Carboxylate O–donors	ChCl–MA	Formation of RE–O coordination species	Enhances selective REE leaching	[111]
	P–O donor ligands	BTMPPA–phenol	Formation of RE–O–P coordination species	Enhances REE extraction selectivity	[104]

BeCl, betaine hydrochloride; BTMPPA, bis(2,4,4-trimethylpentyl)phosphinic acid; CA, citric acid; ChCl, choline chloride; DES, deep eutectic solvent; EG, ethylene glycol; MA, malonic acid; OA, oxalic acid; PPA, phenylphosphinic acid; PTSA, p-toluenesulfonic acid; REE, rare-earth element; $[N_{8881}]Cl$, trioctylmethylammonium chloride.

4. Multiscale Modeling for Mechanistic Interpretation and DES Design

4.1. DFT for Elucidating Local DES Interactions and Metal-Release Mechanisms

DES leaching experiments directly provide macroscopic information on leaching efficiency, selectivity, and kinetics [16,17]. However, these observations often cannot explain the local origins of performance differences [33]. The constituent species of DESs, including hydrogen-bond acceptors (HBAs), hydrogen-bond donors (HBDs), and, where present, ionic components, do not act independently. Instead, they form specific local structures through hydrogen bonding, electrostatic interactions, ionic association, and charge transfer [112,113]. These structures further influence proton activation, solid-state bond cleavage, and metal coordination. Because these processes occur at molecular and interfacial scales, they are difficult to distinguish using conventional leaching experiments. DFT translates such local interactions into comparable structural and energetic information through conformational optimization and electronic-structure analysis [32,33,41]. Relevant descriptors include bond lengths, charge distributions, binding energies, and reaction energies. These results provide a molecular-scale basis for linking DES composition and local structure to leaching behavior.

A key question is how the local structure of a DES interacts with solid-state bonds and ultimately controls metal release. Metals in solid wastes may occur as lattice-embedded, oxide-bound, support-bound, or framework-bound species, each associated with different bond strengths and release barriers [59,114–117]. DFT can optimize the adsorption configurations of DES components on solid surfaces and calculate adsorption energies, bond-length changes, charge transfer, and reaction-energy barriers. These calculations help identify the interfacial interactions and bond-breaking steps that control metal release [32,33]. Hydrogen bonding and ionic interactions among DES components can alter proton activity, ligand electron-donating ability, and interactions with solid surfaces [74,118]. These changes, in turn, affect the stability of key M-O or metal-framework bonds. In a ChCl-oxalic acid system, hydrogen bonding between Cl^- and oxalic acid elongates the O-H bond from 0.982 to 1.074 Å. Meanwhile, the C-O bond shortens from 1.347 to 1.304 Å, indicating substantial electronic reorganization around the carboxylic group [74]. Such changes can propagate to the solid–liquid interface. In a ChCl-urea/CuO system, urea adsorption followed by proton transfer alters the electronic environment around Cu and its binding strength to the oxide surface [119]. By contrast, Al substitution in NCM materials forms stable Al-O bonds that enhance lattice-oxygen stability and modify dissolution behavior in DESs [120]. DFT can therefore relate macroscopic differences in leachability to local electronic-structure changes and the weakening or stabilization of specific chemical bonds.

As research shifts from single-metal systems to realistic multimetal wastes, explaining differences in metal leaching and separation within the same DES becomes increasingly important. Selectivity depends not only on differences in solid-phase release barriers but also on competitive coordination with Cl^-, carboxylates, and other functional sites [36,121]. DFT can compare the binding energies, preferred coordination structures, and competitive complexation strengths of different metal-ligand combinations [122]. These comparisons reveal the relative affinities of metals for specific functional sites and clarify the molecular origins of selectivity. For example, Co, Mn, Li, and Ni exhibit distinct preferred coordination modes in a ChCl-acetic acid system [123]. These differences can subsequently be exploited for stepwise separation. In a ChCl-oxalate-H_2O system, computational analyses revealed competitive coordination among Li^+, Co^{2+}, oxalate, Cl^-, and H_2O (Figure 3a–c) [72]. Experimentally, selective Li leaching was more than one order of magnitude higher than that of Co, Ni, and Mn [72]. These findings show that DFT can evaluate whether a metal is readily stabilized by a specific ligand. It can also relate macroscopic selectivity to differences in metal-ligand interaction strength and dominant solution species.

Overall, DFT translates local structural reorganization, interfacial bond cleavage, and competitive coordination into interpretable structural and energetic information [124]. These processes are otherwise difficult to observe directly during DES leaching. This approach establishes mechanistic links among DES composition, molecular-scale interactions, and macroscopic leaching behavior. However, DFT results remain sensitive to initial configurations, reaction pathways, exchange-correlation functionals, and solvent models [125]. Conventional cluster-based DFT also cannot fully capture the dynamic hydrogen-bond networks, hydration effects, and multicomponent competition present in realistic DES systems [126].

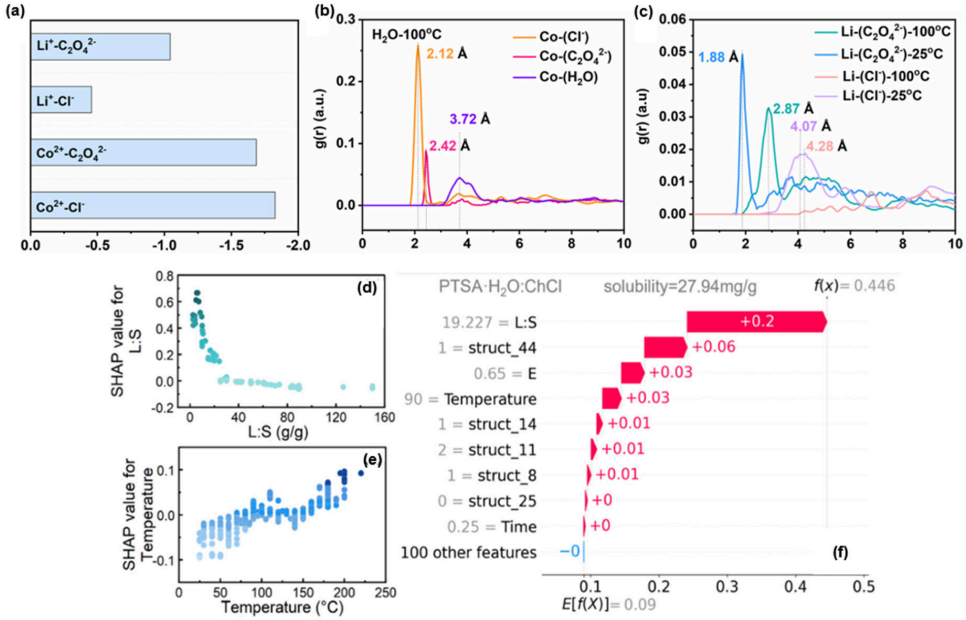


Figure 3. Representative computational approaches for multiscale analysis and screening of DES-based metal recovery systems. (**a**) Calculated interaction energies of Li^+ and Co^{2+} with oxalate and Cl^-. (**b**) Radial distribution functions (RDFs) describing the coordination of Co^{2+} with Cl^-, oxalate, and H_2O at 100 °C. (**c**) RDFs describing the coordination of Li^+ with oxalate and Cl at 25 and 100 °C. Reproduced from Ref. [72] with permission from Elsevier. (**d**) SHAP dependence plot showing the effect of the liquid-to-solid ratio on predicted metal solubility. (**e**) SHAP dependence plot showing the effect of temperature on predicted metal solubility. (**f**) SHAP waterfall plot illustrating the contributions of individual features to the predicted solubility for a representative DES system. Reproduced from Ref. [34] with permission from the Royal Society of Chemistry. Copyright 2024 The Royal Society of Chemistry.

4.2. Predicting Solvation Capacity and Phase-Distribution Behavior with COSMO-RS

DFT can reveal local metal-ligand interactions and key interfacial processes, but local binding strength alone does not determine whether a metal species is thermodynamically stabilized in the overall DES environment or preferentially distributed into a target phase [127,128]. For selective recovery, the unresolved questions are therefore whether a given DES can stabilize the target metal more strongly than alternative solvents, and whether this difference is sufficient to generate selective phase partitioning relative to competing metals [129]. COSMO-RS addresses these questions by using quantum-chemically derived surface screening-charge densities to calculate σ-profiles, σ-potentials, chemical potentials, activity coefficients, and phase-equilibrium properties [35]. It therefore extends local structural information from DFT to bulk solvation and phase-distribution thermodynamics [130].

The large compositional space of DESs makes solvation screening particularly important. Changes in HBA/HBD composition alter polarity, hydrogen-bonding characteristics,

and surface charge distributions, so the same metal species may exhibit markedly different thermodynamic affinities across candidate DESs [131,132]. COSMO-RS can quantify these differences and rank solvents before experimental testing [130]. For example, Amusa et al. [133] screened 675 candidate DESs for $LiCoO_2$-related recovery and reduced the initial solvent space to only a small number of high-potential systems. In another study, σ-surface and σ-potential analyses were used to compare the interaction of TOPO-based hydrophobic DESs with Ce(III), and the systems predicted to be more favorable also showed superior extraction experimentally [134]. These results demonstrate that COSMO-RS can convert DES compositional differences into directly comparable solvation affinities, substantially narrowing the experimental search space.

High solvation affinity, however, does not necessarily translate into selective separation. In multimetal systems, effective recovery requires a sufficiently large difference in the thermodynamic preference of the target and competing metals for the coexisting phases [127,129]. If both species are similarly stabilized in the DES phase, high extraction of the target may still be accompanied by substantial co-extraction. COSMO-RS can evaluate this difference through chemical potentials, activity coefficients, and liquid–liquid equilibrium calculations, thereby predicting whether metal complexes preferentially partition into the DES or aqueous phase [35,128]. This is particularly relevant for hydrophobic DESs, where separation depends on the free-energy difference associated with transferring a metal complex between the two phases [130,132]. Studies of Ce(III) extraction have shown that COSMO-RS-selected hydrophobic DESs can achieve extraction efficiencies above 90% under experimentally favorable conditions [134]. The key value of COSMO-RS is therefore not simply to identify a solvent with strong metal affinity, but to determine whether differences in solvation are large enough to support selective phase transfer.

This thermodynamic description still does not fully predict practical recovery performance. DES viscosity, water content, and non-ideal solution behavior can alter mass transfer, coordination environments, and phase separation, while ion-pair representation, conformational selection, and parameterization directly affect COSMO-RS accuracy [73,126,135–137]. Experimental calibration is therefore required for complex real leachates [125]. More importantly, COSMO-RS predicts thermodynamic preference rather than solid-state bond cleavage, interfacial reaction kinetics, or actual leaching rates [129]. Its greatest strength lies in ranking candidate DESs and predicting solvation and phase-partitioning trends within a predefined chemical space. Once DES composition, operating conditions, and multiple interacting variables must be optimized simultaneously, this predefined thermodynamic screening becomes insufficient, motivating the use of machine-learning approaches for higher-dimensional prediction and optimization [138,139].

4.3. Predicting Leaching Performance Under Multifactor Coupling and Designing Candidate Systems Using Machine Learning

Practical DES-based leaching is jointly governed by solid-waste characteristics, DES structure, and operating conditions [140]. Metal speciation and host phases determine the initial difficulty of release, whereas DES acidity, redox properties, and coordination capacity influence dissolution and stabilization. Water content, viscosity, temperature, liquid-to-solid ratio, and reaction time further regulate mass transfer and reaction kinetics [129]. These variables often interact nonlinearly and are strongly coupled [141,142]. Consequently, single-factor experiments cannot answer a more practical question: which combinations provide higher leaching efficiency and selectivity when material properties, solvent composition, and operating conditions vary simultaneously? Machine learning can integrate solid-waste composition, DES structure and physicochemical properties, DFT/COSMO-RS descriptors, and operating conditions within a unified feature space [140]. Models can then learn their relationships with leaching efficiency, selectivity, and impurity co-leaching. This

approach moves DES optimization beyond single-variable adjustment toward multivariable performance prediction.

Machine learning can also prioritize promising systems that have not been extensively validated experimentally, reducing reliance on exhaustive trial and error. Zhou et al. [34] developed an extreme gradient boosting (XGBoost) model using existing DES-leaching data to predict metal-leaching performance. They further combined the model with a conditional generative adversarial network and identified a ChCl-glycolic acid system with high predicted leaching potential. The selected system was subsequently validated experimentally [34]. Nurfajrin et al. [141] integrated quantum-chemical calculations, COSMO-RS, and machine learning to screen 218 candidate combinations. They identified a 2,2′-bipyridine-phenol DES that achieved extraction efficiencies of 99% for Ni and 97% for Co from simulated waste-battery leachate. Although this study focused on liquid–liquid extraction, it illustrates the broader value of combining theoretical descriptors with machine learning. This strategy can reduce a large candidate space to a few high-performing systems, thereby substantially improving DES-screening efficiency.

The value of machine learning extends beyond identifying high-performing DESs. More importantly, it can identify the variables most strongly associated with predicted leaching behavior, thereby shifting screening towards problem-oriented solvent design. For DES-based leaching, this involves determining which solvent characteristics and operating variables dominate model predictions and whether their effects are nonlinear or interactive. Feature-importance analysis, SHapley Additive exPlanations (SHAP), and partial-dependence analysis can estimate individual feature contributions and visualize interactions among DES composition, solvent properties, and operating conditions (Figure 3d–f). Using an XGBoost–SHAP framework, Zhou et al. [34] identified the liquid-to-solid ratio and temperature as two of the most influential predictors of metal leaching performance. Reaction time, together with the acidity, reducing ability, and coordination capacity of the DES, also contributed substantially to the model predictions. Amusa et al. [140] used an ensemble neural-network model to describe the leaching of spent $LiCoO_2$ using a glycine–ascorbic acid–water DES. The model simultaneously predicted Li and Co leaching behavior. Collectively, these studies show that machine learning can not only predict which systems are likely to perform better but also help identify the variables associated with predicted performance differences. Such information can support the targeted design of DESs for specific solid wastes and target metals.

These predictive and design capabilities, however, depend strongly on the quality and representativeness of the training data. Literature-derived datasets may suffer from publication bias because unsuccessful or low-performing leaching results are less frequently reported. Differences in feedstock composition, pretreatment, operating conditions, and analytical procedures can also introduce substantial inter-study heterogeneity [143–145]. Consequently, high predictive metrics obtained from internal validation do not necessarily indicate reliable extrapolation to unseen waste compositions or complex industrial leachates. A DES-leaching database should contain more than final leaching efficiencies. It should record solid-waste composition and metal occurrence states, DES composition and physicochemical properties, water content, temperature, reaction time, liquid-to-solid ratio, and agitation conditions. Target-metal recovery, impurity co-leaching, and cycling performance should also be documented. DFT-derived descriptors of bonding, adsorption, reaction energetics, and coordination can strengthen the physical basis of the learned structure-performance relationships [146]. COSMO-RS-derived activity coefficients, chemical potentials, solvation properties, and phase-partitioning parameters can provide additional thermodynamic information [147]. Nevertheless, machine learning cannot reliably extrapolate beyond the chemical space represented in the training data. Nor can it replace

mechanistic understanding of solid-state bond cleavage, interfacial mass transfer, or high-solid-loading effects [31,148]. Its most appropriate role is as a high-dimensional prediction and design tool that integrates molecular descriptors, material characteristics, process variables, and experimental validation. Table 5 summarizes representative applications of DFT, COSMO-RS, and machine learning in DES-assisted metal recovery, highlighting their respective roles in molecular interaction analysis, solvent screening, phase-behavior prediction, and performance optimization.

Table 5. Representative multiscale modeling approaches for DES design: key inputs, outputs, and model validation.

Method	Design Task	Key Inputs	Outputs and Representative Validation	Reference
DFT	DES hydrogen bonding and proton activation	Molecular and hydrogen-bonding configurations	Bond-length and electronic-structure changes; consistent with observed hydrogen-bonding and proton-activation behavior	[74]
	Metal/oxide interfacial interactions	Cu/CuO structures, urea species, and Cl^-	Bonding and electronic-structure changes; consistent with dissolution trends	[119]
	NCM lattice stability and Al effects	Al substitution, oxygen vacancies, and solvent adsorption	Bonding and electronic-structure changes; consistent with dissolution trends	[120]
	Multimetal coordination and separation	Metal ions, Cl^-, CH_3COO^-, and acetone	Preferred coordination structures and energy barriers; consistent with Co/Mn-Li/Ni partitioning	[123]
	Water-dependent competitive coordination	Li^+, Co^{2+}, Cl^-, $C_2O_4{}^{2-}$, H_2O, and temperature	Binding energies and RDFs; consistent with preferential $Li_2C_2O_4$ precipitation	[72]
COSMO-RS	Large-scale DES screening	Structures of 15 HBAs, 45 HBDs, and LCO	Activity-coefficient and affinity ranking; 675 combinations reduced to 8 candidates	[133]
	HDES screening for Ce extraction	HDES components and Ce(III) species	σ-surfaces/profiles/potentials; selected system experimentally validated	[134]
ML	Cathode-solubility prediction and DES generation	Molecular fingerprints, DES properties, descriptors, and conditions	Solubility prediction and feature importance; XGBoost R^2 = 0.9702	[34]
	DES formation and Ni/Co selectivity screening	Molecular descriptors and COSMO-RS SLE data	DES formation and selectivity classification; RF/XGBoost scores = 0.72/0.74	[141]

HBA, hydrogen-bond acceptor; HBD, hydrogen-bond donor; HDES, hydrophobic deep eutectic solvent; LCO, lithium cobalt oxide; NCM, nickel-cobalt-manganese; RDF, radial distribution function; RF, random forest; SLE, solid–liquid equilibrium; XGBoost, extreme gradient boosting.

5. Separation and Purification of DES Leachates, Product Recovery, and Solvent Regeneration

High leaching efficiency alone does not guarantee effective metal recovery, as downstream separation and DES regeneration determine product recoverability and solvent recyclability [23,41]. The integrated pathway from selective separation to product formation, DES regeneration, and solvent return is illustrated in Figure 4 Table 6 summarizes representative recovery routes, product quality, solvent reuse/regeneration strategies, and cycling performance. In this context, reuse denotes repeated use of recovered DES without demonstrated restoration of its original composition, whereas regeneration involves restoration or adjustment of solvent composition and functionality.

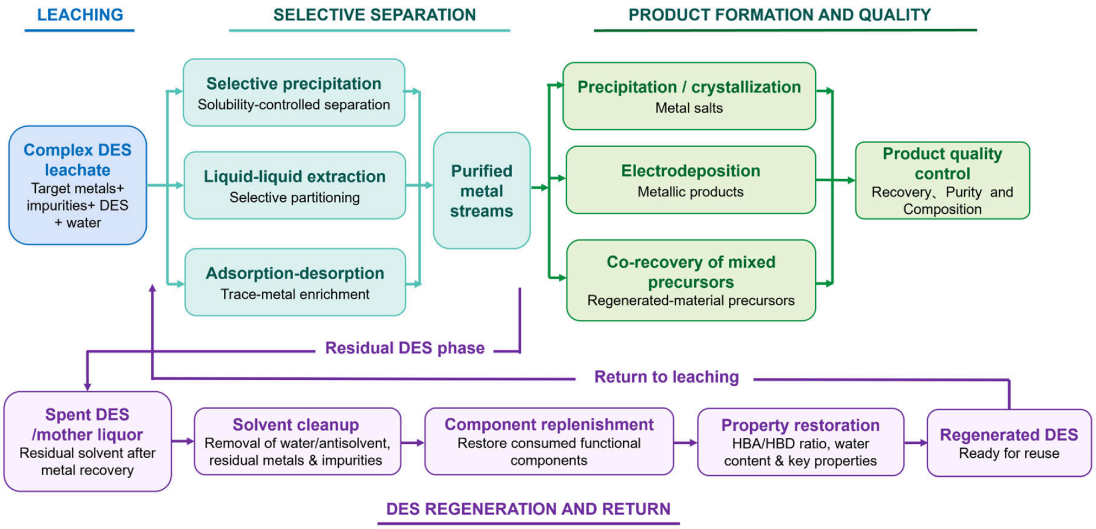


Figure 4. Integrated separation and recovery pathway following DES-assisted metal leaching, including selective separation, product formation, DES regeneration, and solvent reuse.

Table 6. Representative product recovery and DES regeneration strategies in DES-based metal recovery systems.

Treatment Category	Recovery Method	Feed/Leachate	DES System	Target Metal(s)	Recovery Rate	Product	Purity	DES Reuse/ Regeneration Strategy	Cycling Performance	Reference
Precipitation/ crystallization	Stepwise precipitation by water-content control	Leachate from spent $LiCoO_2$ cathode active material	ChCl-OA-H_2O	Li Co	90.0% 94.6%	$Li_2C_2O_4$ $CoC_2O_4{\cdot}2H_2O$	98.43% 99.89%	Replenishment of ChCl and OA; water-content adjustment	Performance remained essentially stable after 3 cycles	[72]
	Ethanol-induced stepwise precipitation	Leachate from spent NCM cathode material	BeCl-CAA	Li Ni Co Mn	86.10% 98.78% 93.15% 91.97%	Li_2CO_3 $NiC_2O_4{\cdot}2H_2O$ $CoC_2O_4{\cdot}2H_2O$ $Mn(OH)_2$	NR	NR	NR	[149]
	Selective phosphate precipitation	Leachate from model $LiCoO_2$ cathode	ChCl-H_3PO_4	Li Co	NR 79%	Li_3PO_4 $(CoHPO_4)_2{\cdot}3H_2O$	97.5% 99.3%	Ethanol evaporation and reuse	Li and Co leaching efficiencies remained at 94.3% and 80.8% after 5 cycles	[86]
	Closed-loop oxalate precipitation	Leachate from spent $LiCoO_2$ cathode material	MA-EG	Co Li	>96.5% 80.4%	$CoC_2O_4{\cdot}2H_2O$ $Li_2C_2O_4$	NR	Oxalic-acid replenishment and reuse	Co leaching efficiency remained at 90% after 4 cycles	[150]
Electrochemical recovery	Sequential potentiostatic electrodeposition	NCM111 and NCM811 leachates	ChCl-EG	Ni Co Mn	>95%	Ni Co Mn	NCM111: 99.1%, 96.3%, NR; NMC811: 99.2%, 98.8%, NR	Water removal by evaporation and reuse	Performance remained essentially stable over 4 cycles	[151]
	Sequential separation and electrodeposition	Spent NCM811 cathode material	ChCl-EG-TA	Li Co Ni	99.9% 98.1% 95.6%	Li_2CO_3 $Co(OH)_2$ NiO	98.4% 97.3% 96%	Water removal by heating	Ni recovery and product purity remained above 90% after 3 cycles	[152]
Precursor /material regeneration	Antisolvent crystallization and cathode regeneration	NCM111 leachate	ChCl-L-(+)-tartaric acid	Co Ni Mn	>96%	Mixed Ni/Co/Mn tartrate precursor; regenerated NMC material	NR	NR	NR	[153,154]

Table 6. *Cont.*

Treatment Category	Recovery Method	Feed/Leachate	DES System	Target Metal(s)	Recovery Rate	Product	Purity	DES Reuse/ Regeneration Strategy	Cycling Performance	Reference
Integrated recovery	Integrated delamination-filtration-precipitation	$LiCoO_2$ cathode sheets with Al foil	ChCl-malonic acid-2-pyrrolidone	Co Li	93.4% 83.7%	$CoC_2O_4 \cdot 2H_2O$ Li_2CO_3	NR	Water removal by evaporation and reuse	Co leaching efficiency remained >90% after 4 cycles	[155]
	In situ precipitation coupled with solvent recovery	$LiCoO_2$ and NCM cathode materials	EG-EtOH-CA	Co Li	NR 100%	$CoC_2O_4 \cdot 2H_2O$ Li_2CO_3	NR	Solvent evaporation and reuse	Li leaching efficiency remained >90% after 5 cycles	[70]
	Rotary evaporation with component replenishment	Leachate from spent NCM622 cathode material	$[N_{2222}][Cl]$-PA	Ni Co Mn Li	NR	$(Ni,Co,Mn)C_2O_4 \cdot 2H_2O$ mixed precursor; $Li_2C_2O_4$	NR	Water removal and PA replenishment	Li, Ni, Co, and Mn leaching efficiencies all remained >95% after 5 cycles	[41]

BeCl, betaine hydrochloride; CA, citric acid; CAA, chloroacetic acid; ChCl, choline chloride; DES, deep eutectic solvent; EG, ethylene glycol; EtOH, ethanol; MA, maleic acid; NCM, nickel–cobalt–manganese; OA, oxalic acid; PA, pyruvic acid; TA, tartaric acid; $[N_{2222}][Cl]$, tetraethylammonium chloride; NR, not reported.

5.1. Leachate Characteristics and Selection of Separation Pathways

When compositionally complex solid wastes are treated with DESs, both target metals and impurities, including Fe, Cu, and Al, may enter the liquid phase. The resulting leachate may also contain DES components, water, residual reagents, and fine particles [156]. Variations in water content and residual acidic or redox-active species may further alter metal coordination and valence-state equilibria [157,158]. Accordingly, separation strategies for complex DES leachates cannot be designed solely on the basis of metal concentrations. They must also account for differences in valence state, coordination stability, solubility, and phase affinity [159]. Metals with pronounced solubility differences or strong tendencies to form sparingly soluble species can be separated by selective precipitation [160]. Metals that remain as soluble complexes can be separated by liquid–liquid extraction according to their phase affinities [30,130,132]. Residual metals present at low concentrations can then be further enriched through adsorption–desorption.

Selective precipitation separates metals by adjusting their valence states or promoting the formation of sparingly soluble species [160]. It is particularly suitable for the rapid separation of relatively concentrated metal components. However, high precipitation recovery does not necessarily indicate high product quality. Carreira et al. [161] treated a TOPO-decanoic acid DES system with $KMnO_4$, achieving approximately 98% Mn recovery but only 81% purity for the resulting Mn_3O_4. This comparison shows that impurity coprecipitation can markedly reduce product purity, even when most of the metal has been removed from the liquid phase. Precipitation should therefore be evaluated using metal recovery, target-metal loss, and precipitate purity rather than liquid-phase metal removal alone.

For metals that coexist as soluble complexes, liquid–liquid extraction can translate differences in coordination behavior into differences in phase partitioning [30,130,132]. Following extraction of an automotive-catalyst DES leachate, Pt, Pd, and Rh transferred nearly quantitatively to the extract phase, whereas approximately 80% of Al remained in the original leachate [162]. This result shows that differences in complex phase affinity can selectively separate precious metals from support-derived elements. When target-metal concentrations become too low for efficient liquid–liquid extraction, adsorption–desorption can provide further enrichment based on interfacial affinity. For example, mica recovered up to approximately 97% of Nd from a salicylic acid-ChCl leachate and remained reusable after desorption with $CaCl_2$ [163].

Selective precipitation, liquid–liquid extraction, and adsorption–desorption should not be considered treatment steps with a fixed sequence. Instead, they exploit differences in solubility, phase affinity, and interfacial adsorption to separate metals across different concentration ranges and speciation conditions. In practice, these methods should be selected or combined according to the leachate composition, metal coordination forms, and target-product requirements. Such combinations enable the stepwise fractionation and enrichment of co-leached components [23].

Following liquid-phase separation, the enriched metals must be converted into salts, precursors, or metallic products with defined compositions, purities, and intended uses [31]. Product recovery from DES leachates can follow three main routes, depending on metal solubility, electrochemical properties, and the desired product form [164]. These routes comprise precipitation or crystallization of metal salts, electrochemical reduction to metallic products, and co-recovery of mixed precursors without complete metal separation. Because DESs differ from aqueous solutions in coordination environment, ionic activity, and mass transfer, established aqueous operating conditions cannot be transferred directly [126]. Each route must instead be controlled according to product yield, purity, composition, and application performance.

5.2. Product Recovery and Quality Control

When target metals form sufficiently insoluble salts, selective precipitation and crystallization can be induced by adjusting the DES composition or water content [165]. In a ChCl-oxalic acid system, Li first precipitated as $Li_2C_2O_4$. Water addition to the resulting Co-rich filtrate then yielded $CoC_2O_4{\cdot}2H_2O$, with recovery efficiencies above 90% for both metals [135]. In a ChCl-H_3PO_4 system, Li_3PO_4 and $(CoHPO_4)_2{\cdot}3H_2O$ were obtained at product purities of 97.5% and 99.3%, respectively [86]. These findings indicate that functional DES components can support leaching while also supplying the anions required for product formation. The solvent can therefore contribute directly to the product-recovery stage. Nevertheless, precipitation recovery does not fully represent overall metal recovery. Metal losses during filtration, washing, and intermediate liquid transfer must be evaluated separately from final product purity [166].

For electrochemically reducible metals, electrodeposition can directly produce metallic products while reducing the demand for additional precipitants [164]. However, deposition behavior is jointly governed by applied potential, coordination environment, and mass transfer [31]. In a real NMC leachate, adjusting the water content and deposition potential produced recovery efficiencies above 95% for both Ni and Co [151]. In more compositionally complex black-mass leachates, Cu and Co retained relatively high deposition efficiencies, whereas Ni deposition decreased substantially [167]. This contrast shows that standard electrode potentials alone cannot determine deposition sequences in real DES systems. Competitive coordination, ionic activity, and mass-transfer limitations also influence selective deposition and final recovery.

When the final objective is to regenerate multimetal materials, complete separation of individual metals may be unnecessary. Instead, multiple leachate components can be co-converted into mixed precursors. In a ChCl-tartaric acid leachate, ethanol antisolvent crystallization recovered approximately 98.5% of the transition-metal tartrates [153]. Related work further demonstrated that mixed precursors obtained through this route could be used to resynthesize NMC materials [154]. This route reduces the need to separate individual transition metals completely. However, Li partitioning and the coprecipitation of Al and Cu may alter precursor stoichiometry and consequently affect the performance of the regenerated material.

Precipitation or crystallization, electrodeposition, and mixed-precursor recovery should not be regarded as treatment steps with a fixed sequence. Rather, they serve different product objectives, including metal salts, metallic products, and precursors for material regeneration [166]. The appropriate pathway should be selected according to metal speciation, desired product form, and downstream use. Performance should be evaluated beyond liquid-phase metal removal by considering product recovery, phase composition, purity, stoichiometry, crystallinity, residual impurities, and final application performance [168].

5.3. DES Regeneration and Closed-Loop Operation of the Overall Process

Maintaining high leaching efficiency over repeated cycles does not necessarily indicate that a DES has been restored to its initial state [169]. During cycling, functional-component depletion, changing water content, impurity accumulation, and chemical or thermal degradation of DES components may progressively alter solvent composition, physicochemical properties, and reactivity [31,170]. Such degradation may modify hydrogen-bonding interactions, viscosity, acidity, and coordination behavior even before an obvious decline in leaching efficiency is observed. Evaluating DES cycling therefore requires more than confirming the retention of leaching performance. It must also determine whether solvent

composition and key physicochemical properties are restored and quantify the material and energy inputs required to maintain performance [126,171,172].

Existing studies have emphasized performance retention far more than restoration of the solvent state. After Ni, Mn, and Co were precipitated from an ethaline leachate by adding water, the added water was subsequently removed. The recovered DES could then support at least three additional leaching cycles without an obvious decline in performance [173]. However, this result demonstrates only reuse or partial solvent recovery, not restoration of the HBA/HBD ratio, water content, or residual-metal concentration. When leaching consumes functional components, removing water alone is even less likely to restore solvent functionality. In a Cys-LA DES, cysteine consumed through oxidation had to be replenished after each cycle to maintain high Co recovery over three cycles [174]. This dependence shows that stable cycling requires restoration of functional components rather than simple recovery of the mother liquor. Even after solvent recovery or compositional adjustment, performance losses may differ among metals. After five cycles in a ChCl-H_3PO_4 system, Li and Co leaching efficiencies remained at 94.3% and 80.8%, respectively [86]. This contrast indicates that individual metals respond differently to changes in solvent composition and impurity accumulation [175]. Leaching efficiency during cycling therefore indicates only whether DES functionality has been temporarily retained. Demonstrating regeneration also requires monitoring the HBA/HBD ratio, water content, residual-metal concentration, viscosity, acidity, and redox capacity.

Restoration of solvent composition and performance must also be assessed against the associated material and energy costs [176]. DES regeneration commonly involves evaporation, heating, replenishment of functional components, and other auxiliary treatments [177]. Repeated thermal treatment may also promote component decomposition or secondary reactions, thereby changing DES composition and potentially increasing the replenishment demand [178]. These operations may offset the environmental benefits of solvent recycling. In an ethaline-based electrochemical recovery system, metal-recovery performance remained relatively stable over four consecutive cycles. Nevertheless, water evaporation and operation at 85 °C accounted for approximately 98.4% of total energy consumption [151]. This result shows that a larger number of reuse cycles does not necessarily reduce environmental burdens. Closed-loop DES operation should therefore be evaluated using both metal and solvent mass balances. Relevant metrics include performance degradation, DES recovery, component loss and replenishment, impurity accumulation, regeneration energy demand, and newly generated waste streams. In this review, substantive closed-loop regeneration is achieved only when solvent functionality is restored and regeneration reduces the overall material consumption and environmental burden of the entire recovery process.

6. Sustainability and Engineering Feasibility

The preceding sections examined DES leaching mechanisms, solvent design, metal separation, product recovery, and solvent regeneration. However, high leaching rates or stable short-term cycling do not directly demonstrate sustainability or industrial applicability [41,179]. A comprehensive evaluation of DES-based processes must address three questions. Does the overall process reduce environmental impacts. Can revenue from metal recovery offset solvent and processing costs. Can laboratory-scale systems remain stable under scaled-up and continuous operating conditions. Accordingly, this section evaluates the practical feasibility of DES-based metal recovery from solid waste through life-cycle assessment, techno-economic analysis, and engineering implementation [41]. Table 7 summarizes the major evaluation dimensions, assessment methods, and key metrics required to evaluate the sustainability and engineering feasibility of DES-based metal recovery processes.

Table 7. Evaluation framework for the sustainability and engineering feasibility of DES-based metal recovery processes.

Evaluation Dimension	Primary Method	Key Metrics and Considerations	References
Environmental sustainability	Life-cycle assessment (LCA)	GWP, resource and energy use, toxicity, functional unit and system boundary, product purity/recovery level, and uncertainty analysis	[180]
Economic feasibility	Techno-economic analysis (TEA), sensitivity analysis, and break-even analysis	CAPEX, OPEX, unit treatment cost, product revenue, DES price and consumption, solvent lifetime, and processing scale	[181,182]
Resource and circular efficiency	Material flow analysis (MFA) and energy balance	Overall metal recovery, DES recovery and component losses, replenishment requirements, waste generation, and performance retention over reuse cycles	[31]
Engineering scalability	Scale-up and continuous-operation validation	Solid loading, throughput, mass-transfer efficiency, energy consumption per unit product, and continuous-operation stability	[17,110]
Process safety	Process hazard analysis (PHA) and materials compatibility testing	Corrosion and material compatibility, thermal stability, gas-release risks, occupational exposure, and long-term operational safety	[110,183]

6.1. Life-Cycle Assessment, Toxicity, and Environmental Sustainability

Low volatility may reduce direct solvent emissions, but it does not by itself establish a lower environmental impact for DES-based recovery processes. The overall environmental performance depends on material and energy inputs across the full process, including DES production, reagent consumption, solvent losses, regeneration, and downstream processing [126,184]. Environmental assessment should therefore address upstream burdens from DES feedstock production and solvent consumption. It should also quantify energy and reagent demands from separation, product recovery, and solvent regeneration. A complete assessment must further include non-carbon impacts, such as toxicity, biodegradability, water use, and residual contamination. Accordingly, LCA requires consistent functional units and system boundaries [180,185]. Meaningful comparisons should also consider product purity and recovery basis, together with uncertainty in key parameters such as solvent lifetime, regeneration efficiency, and energy demand. The assessment should integrate DES preparation, leaching, separation and purification, product recovery, solvent regeneration, and waste-stream treatment within a unified framework [174,186].

Existing studies identify DES feedstock production and solvent consumption as major determinants of life-cycle environmental performance [187]. For example, an LCA of a ChCl-formic acid system identified ChCl and formic acid inputs as the dominant contributors to the overall environmental burden [188]. This finding positions lower solvent use, greater DES recovery, and optimized feedstock sourcing as key routes to improved environmental performance. Low volatility and relatively mild operating conditions can reduce burdens at selected process stages. These advantages become stronger when combined with low solvent demand and efficient solvent recovery.

Downstream separation and regeneration determine whether the advantages achieved during leaching extend across the full process [189]. Neutralization, extraction, precipitation, washing, and evaporative regeneration add energy and reagent demands. By contrast, high-quality regenerated products can provide environmental credits by displacing virgin-material production [190,191]. Whole-process performance therefore reflects the balance among front-end leaching, downstream product recovery, and solvent regener-

ation. Key optimization priorities include reducing high-burden operations, increasing product-substitution value, and improving solvent-circulation efficiency.

A complete environmental profile also includes impacts beyond global warming potential and energy consumption. HBAs and HBDs differ substantially in toxicity, biodegradability, water demand, and upstream production burdens [187]. Their performance should therefore be assessed from full production and use profiles rather than feedstock origin alone. Future LCAs can incorporate water consumption, human toxicity, ecotoxicity, DES degradation products, and residual metals in recycled solvents. Sensitivity and uncertainty analyses can then identify the dominant environmental drivers associated with DES recovery, cycle life, energy mix, and product-substitution ratio [192].

6.2. Techno-Economic Feasibility and Key Drivers

The economic competitiveness of DES-based processes is determined by solvent expenditure, process complexity, and the value of the final products [188]. TEA should quantify solvent costs through DES price, liquid-to-solid ratio, replenishment demand, and cycle life. It should also account for energy and reagent expenditures during separation and regeneration, together with the economic contributions of product yield, purity, and added value. Collectively, these factors determine whether laboratory-scale leaching performance can be translated into a competitive industrial recovery route.

DES consumption is often a major cost variable. Lower liquid-to-solid ratios reduce solvent demand per unit of waste while simultaneously decreasing heating and regeneration loads [193]. Higher solid loading, however, places greater demands on viscosity control and mass transfer [194]. The most favorable operating window therefore balances solvent consumption, mass-transfer efficiency, and metal recovery instead of maximizing a single performance metric.

Downstream process complexity also directly influences overall profitability [195]. Multimetal leaching increases the amount of resource transferred into the liquid phase, but its economic value depends on the required separation steps and resulting product value [196]. Byproduct recovery should likewise be evaluated by comparing additional product revenue with the associated separation and purification costs. Selective leaching, direct precursor recovery, and material regeneration provide attractive routes for reducing separation steps while preserving greater product value. These routes offer alternatives to complete leaching followed by sequential purification.

The economic advantage of DES-based processes is therefore driven primarily by high selectivity, low solvent consumption, simplified downstream processing, and high-value final products. Future TEAs can use sensitivity and break-even analyses to identify critical thresholds for DES price, liquid-to-solid ratio, cycle life, product recovery, and processing scale [197]. These thresholds can define the technical and market conditions under which DES-based systems achieve economic competitiveness.

6.3. Process Intensification, Engineering Scale-Up, and Safe Implementation

The engineering value of DES-based processes rests on mass-transfer and rheological performance, long-term operational stability, and equipment and process safety. High viscosity affects agitation, pumping, particle suspension, and solid–liquid separation [198]. During extended cycling, accumulated metals, auxiliary reagents, and degradation products progressively alter solvent composition and reactivity [199]. Acidic components, Cl^-, and strongly oxidizing conditions place additional demands on equipment materials and process safety [200]. Engineering assessment should therefore quantify mass-transfer efficiency, stability under continuous operation, throughput, unit energy demand, and material compatibility.

Mass-transfer and rheological behavior provide the foundation for DES scale-up [198]. Increasing water content, raising temperature, or intensifying mixing can improve metal release under laboratory conditions. At larger scale, these variables also determine energy requirements for pumping, mixing, heating, solid–liquid separation, and solvent regeneration. Rheological evaluation should cover the operating ranges of water content, temperature, metal loading, and cycling state [132,199]. It should also report the associated energy demand per unit of waste treated or product recovered.

Continuous operation depends on controlling time-dependent changes in DES composition and performance. The accumulation of residual metals, auxiliary components, and degradation products can modify viscosity, acidity, coordination capacity, and selectivity [174]. Short-term cycling establishes immediate reuse performance, while engineering validation extends this assessment to prolonged operation. Tracking these solvent parameters together with product quality over time enables the stable operating window of the DES system to be defined directly.

The engineering value of process-intensification technologies must likewise be assessed at the relevant scale. Microwave irradiation, ultrasound, and mechanochemical processing can substantially enhance mass transfer and reaction rates. For example, some microwave-assisted DES systems achieve high metal release within minutes [201]. At engineering scale, their competitiveness depends on throughput, energy-conversion efficiency, heating uniformity, and energy consumption per unit of product. Corrosive components and strongly oxidizing conditions also increase performance requirements for reactors, piping, seals, and filtration materials [200]. These requirements directly influence safety, capital expenditure, and operating costs. Pilot-scale DES systems should therefore integrate continuous-operating stability, throughput, unit energy consumption, material compatibility, and safety within the same evaluation framework.

Overall, engineering evaluation of DES-based recovery should prioritize the stable production of high-quality products within acceptable limits of material consumption, energy demand, and safety. Complete laboratory-scale mass and energy balances should include DES losses, auxiliary-reagent consumption, product yield, and waste-stream generation [179,202]. These balances provide the quantitative foundation for subsequent LCA, TEA, and engineering scale-up.

7. Conclusions and Outlook

This review establishes an analytical framework that integrates metal occurrence states, initial release barriers, DES-assisted leaching mechanisms, multiscale solvent design, and whole-process resource recovery. The framework begins with how target metals occur within the solid matrix, identifies the dominant barriers that must be overcome during transfer into the liquid phase, and then interprets the relative roles of proton activation, redox regulation, coordination stabilization, and mass transfer. On this basis, DFT, COSMO-RS, and machine learning support mechanistic understanding and rational DES design from the perspectives of local bonding, bulk solvation and phase distribution, and multivariable performance prediction, respectively. The framework further incorporates selective separation, product recovery, DES regeneration, and environmental, economic, and engineering evaluation within a unified system.

This framework indicates that DES leaching performance is governed less by the isolated enhancement of acidity, redox capacity, or coordination strength than by the matching between dominant release barriers and DES functions. Different occurrence states exhibit distinct bonding environments, valence characteristics, and interfacial accessibility, and therefore differ in their requirements for surface activation, phase transformation, bond weakening, electron transfer, and stabilization of dissolved species. These effects are

not related through simple one-to-one correspondence, but often act cooperatively during metal release. DES design should therefore begin with identification of the dominant release barrier and then tailor the relative contributions and coupling of different solvent functions to the characteristics of the target solid waste.

Future research should establish quantitative relationships among solid-phase characteristics, release barriers, DES functions, and process performance that are both interpretable and predictive. Standardized datasets should simultaneously record metal occurrence states, DES composition and water content, operating conditions, target-metal selectivity over impurities, product yield and purity, and DES cycling performance, thereby supporting closer integration among experiments, DFT, COSMO-RS, and machine learning. DES research should also progress from optimization of a single leaching step toward coordinated design of leaching, selective separation, product recovery, and solvent regeneration. Combined with material and energy balances, life-cycle assessment, techno-economic analysis, and engineering scale-up, this approach can provide a more complete basis for evaluating process competitiveness. Through this transition, DESs can advance from leaching media developed for specific wastes toward designable, recyclable, and scalable platforms for recovering resources from complex metal-containing solid wastes.

Author Contributions: Conceptualization, L.W. and A.L.; data curation, E.X.; formal analysis, E.X.; writing—original draft preparation, M.W.; writing—review and editing, M.W., L.W., E.X., A.L. and Y.X.; supervision, A.L.; project administration, Y.X.; resources, Y.X. All authors have read and agreed to the published version of the manuscript.

Funding: This research was funded by the National Science and Technology Major Project, grant number 2025ZD1701406, and the Fundamental Research Funds for the Central Universities, grant number ZY2601.

Data Availability Statement: No new data were created or analyzed in this study. Data sharing is not applicable to this article.

Conflicts of Interest: The authors declare no conflicts of interest.

References

1. Hund, K.; La Porta, D.; Fabregas, T.P.; Laing, T.; Drexhage, J. *Minerals for Climate Action: The Mineral Intensity of the Clean Energy Transition*; Climate-Smart Mining Facility; World Bank: Washington, DC, USA, 2020; p. 112.
2. International Energy Agency. *Global Critical Minerals Outlook 2024*; International Energy Agency: Paris, France, 2024.
3. Baldé, C.P.; Kuehr, R.; Yamamoto, T.; McDonald, R.; D'Angelo, E.; Althaf, S.; Bel, G.; Deubzer, O.; Fernandez-Cubillo, E.; Forti, V.; et al. *The Global E-Waste Monitor 2024*; International Telecommunication Union (ITU): Geneva, Switzerland; United Nations Institute for Training and Research (UNITAR): Bonn, Germany, 2024.
4. Harper, G.; Sommerville, R.; Kendrick, E.; Driscoll, L.; Slater, P.; Stolkin, R.; Walton, A.; Christensen, P.; Heidrich, O.; Lambert, S.; et al. Recycling Lithium-Ion Batteries from Electric Vehicles. *Nature* **2019**, *575*, 75–86. [CrossRef]
5. Işıldar, A.; Rene, E.R.; Van Hullebusch, E.D.; Lens, P.N.L. Electronic Waste as a Secondary Source of Critical Metals: Management and Recovery Technologies. *Resour. Conserv. Recycl.* **2018**, *135*, 296–312. [CrossRef]
6. Xue, Y.; Liu, X. Detoxification, Solidification and Recycling of Municipal Solid Waste Incineration Fly Ash: A Review. *Chem. Eng. J.* **2021**, *420*, 130349. [CrossRef]
7. Piatak, N.M.; Parsons, M.B.; Seal, R.R. Characteristics and Environmental Aspects of Slag: A Review. *Appl. Geochem.* **2015**, *57*, 236–266. [CrossRef]
8. Marafi, M.; Stanislaus, A. Spent Hydroprocessing Catalyst Management: A Review. *Resour. Conserv. Recycl.* **2008**, *53*, 1–26. [CrossRef]
9. Graedel, T.E.; Allwood, J.; Birat, J.-P.; Buchert, M.; Hagelüken, C.; Reck, B.K.; Sibley, S.F.; Sonnemann, G. What Do We Know about Metal Recycling Rates? *J. Ind. Ecol.* **2011**, *15*, 355–366. [CrossRef]
10. Cui, J.; Zhang, L. Metallurgical Recovery of Metals from Electronic Waste: A Review. *J. Hazard. Mater.* **2008**, *158*, 228–256. [CrossRef]
11. Velázquez-Martínez, O.; Valio, J.; Santasalo-Aarnio, A.; Reuter, M.; Serna-Guerrero, R. A Critical Review of Lithium-Ion Battery Recycling Processes from a Circular Economy Perspective. *Batteries* **2019**, *5*, 68. [CrossRef]

12. Tuncuk, A.; Stazi, V.; Akcil, A.; Yazici, E.Y.; Deveci, H. Aqueous Metal Recovery Techniques from E-Scrap: Hydrometallurgy in Recycling. *Miner. Eng.* **2012**, *25*, 28–37. [CrossRef]
13. Ordoñez, J.; Gago, E.J.; Girard, A. Processes and Technologies for the Recycling and Recovery of Spent Lithium-Ion Batteries. *Renew. Sustain. Energy Rev.* **2016**, *60*, 195–205. [CrossRef]
14. Ma, Y.; Wan, J.; Tang, H.; Zhang, Y.; Chen, Z.; Chen, X.; Wei, K.; Shi, Z.; Ma, W. Green Physical Metallurgy Approach for Capturing Silver from Waste Silicon Photovoltaic Cells Using a Tin-bismuth Melt. *Chem. Eng. J.* **2026**, *545*, 179598. [CrossRef]
15. Wang, G.; Yang, Y.; Zhou, S.; Li, B.; Wei, Y.; Wang, H. Data Analysis and Prediction Model for Copper Matte Smelting Process. *Metall. Mater. Trans. B* **2024**, *55*, 2552–2567. [CrossRef]
16. Smith, E.L.; Abbott, A.P.; Ryder, K.S. Deep Eutectic Solvents (DESs) and Their Applications. *Chem. Rev.* **2014**, *114*, 11060–11082. [CrossRef]
17. Hansen, B.B.; Spittle, S.; Chen, B.; Poe, D.; Zhang, Y.; Klein, J.M.; Horton, A.; Adhikari, L.; Zelovich, T.; Doherty, B.W.; et al. Deep Eutectic Solvents: A Review of Fundamentals and Applications. *Chem. Rev.* **2021**, *121*, 1232–1285. [CrossRef]
18. Dai, Y.; Van Spronsen, J.; Witkamp, G.-J.; Verpoorte, R.; Choi, Y.H. Natural Deep Eutectic Solvents as New Potential Media for Green Technology. *Anal. Chim. Acta* **2013**, *766*, 61–68. [CrossRef]
19. Abbott, A.P.; Capper, G.; Davies, D.L.; Rasheed, R.K.; Tambyrajah, V. Novel Solvent Properties of Choline Chloride/Urea Mixtures. *Chem. Commun.* **2003**, *39*, 70–71. [CrossRef]
20. Abbott, A.P.; Capper, G.; Davies, D.L.; McKenzie, K.J.; Obi, S.U. Solubility of Metal Oxides in Deep Eutectic Solvents Based on Choline Chloride. *J. Chem. Eng. Data* **2006**, *51*, 1280–1282. [CrossRef]
21. Peeters, N.; Binnemans, K.; Riaño, S. Solvometallurgical Recovery of Cobalt from Lithium-Ion Battery Cathode Materials Using Deep-Eutectic Solvents. *Green Chem.* **2020**, *22*, 4210–4221. [CrossRef]
22. Tran, M.K.; Rodrigues, M.-T.F.; Kato, K.; Babu, G.; Ajayan, P.M. Deep Eutectic Solvents for Cathode Recycling of Li-Ion Batteries. *Nat. Energy* **2019**, *4*, 339–345. [CrossRef]
23. Moradi, F.; Bougie, F. A Review of the Application of Deep Eutectic Solvents for Metal Recovery from Diverse Secondary Sources. *J. Mol. Liq.* **2026**, *443*, 128903. [CrossRef]
24. Zhang, T.; Dao, J.; Wang, J.; Wan, R.; Li, C.; Wang, D.; Bao, C.; Zhang, Y.; Zhang, Z.; Dong, P. Efficient Leaching of Valuable Metals from NCM Cathode Materials by Green Deep Eutectic Solvent. *J. Clean. Prod.* **2024**, *438*, 140636. [CrossRef]
25. Güloglu, E.; Ilhan, S.; Yardimci, H.; Kalpakli, A.; Zoraga, M.; Orhan, G. Leaching Behavior and Kinetic Modeling of Spent Ni-Mo HDS Catalyst in Deep Eutectic Solvent. *J. Sustain. Metall.* **2026**, *12*, 169–183. [CrossRef]
26. Iondrive Limited. *Consolidated Financial Report for the Half Year Ended 31 December 2025*; Iondrive Limited: Adelaide, SA, USA, 2026; p. 23.
27. Iondrive Limited. *Quarterly Activities Report for the Reporting Period Ended 31 December 2025*; Iondrive Limited: Adelaide, SA, USA, 2026; p. 11.
28. Guo, M.; Deng, R.; Gao, M.; Xu, C.; Zhang, Q. Sustainable Recovery of Metals from E-Waste Using Deep Eutectic Solvents: Advances, Challenges, and Perspectives. *Curr. Opin. Green Sustain. Chem.* **2024**, *47*, 100913. [CrossRef]
29. Yang, C.; Zhao, J.; Mu, P.; Jiang, G.; Tan, Z.; Zhang, X.; Pan, D. Research on Extraction of Valuable Metals from Solid Waste by Deep Eutectic Solvents—A Review. *Process Saf. Environ. Prot.* **2025**, *197*, 107008. [CrossRef]
30. Wang, C.; Zhou, Z.; Zhang, X.; Guo, H.; Boczkaj, G. Metal Extraction Using Deep Eutectic Solvents for Metal Recovery and Environmental Remediation—A Review. *Sep. Purif. Technol.* **2025**, *364*, 132533. [CrossRef]
31. Svärd, M.; Ma, C.; Forsberg, K.; Schiavi, P.G. Addressing the Reuse of Deep Eutectic Solvents in Li-Ion Battery Recycling: Insights into Dissolution Mechanism, Metal Recovery, Regeneration and Decomposition. *ChemSusChem* **2024**, *17*, e202400410. [CrossRef]
32. Tolmachev, D.; Lukasheva, N.; Ramazanov, R.; Nazarychev, V.; Borzdun, N.; Volgin, I.; Andreeva, M.; Glova, A.; Melnikova, S.; Dobrovskiy, A.; et al. Computer Simulations of Deep Eutectic Solvents: Challenges, Solutions, and Perspectives. *Int. J. Mol. Sci.* **2022**, *23*, 645. [CrossRef]
33. Behnajady, B.; Seyf, J.Y.; Karimi, S.; Moradi, M.; Sohrabi, M. Molecular Dynamic (MD) Simulation and Density Function Theory (DFT) Calculation Relevant to Green Leaching of Metals from Spent Lithium-Ion Battery Cathode Materials Using Glucose-Based Deep Eutectic Solvent (DES). *Hydrometallurgy* **2024**, *223*, 106223. [CrossRef]
34. Zhou, F.; Shi, D.; Mu, W.; Wang, S.; Wang, Z.; Wei, C.; Li, R.; Mu, T. Machine Learning Models Accelerate Deep Eutectic Solvent Discovery for the Recycling of Lithium-Ion Battery Cathodes. *Green Chem.* **2024**, *26*, 7857–7868. [CrossRef]
35. Diedenhofen, M.; Klamt, A. COSMO-RS as a Tool for Property Prediction of IL Mixtures—A Review. *Fluid Phase Equilib.* **2010**, *294*, 31–38. [CrossRef]
36. Gao, W.; Nie, C.; Li, L.; Yan, S.; Zhou, W.; Zhu, X. Sustainable and Efficient Deep Eutectic Solvents in Recycling of Spent Lithium-Ion Batteries: Recent Advances and Perspectives. *J. Clean. Prod.* **2024**, *464*, 142735. [CrossRef]
37. Zhu, A.; Bian, X.; Han, W.; Cao, D.; Wen, Y.; Zhu, K.; Wang, S. The Application of Deep Eutectic Solvents in Lithium-Ion Battery Recycling: A Comprehensive Review. *Resour. Conserv. Recycl.* **2023**, *188*, 106690. [CrossRef]

38. Panda, P.; Mishra, S. Deep Eutectic Solvents: Physico-Chemical Properties and Their Use for Recovery of Metal Values from Waste Products. *J. Mol. Liq.* **2023**, *390*, 123070. [CrossRef]
39. Kovacevic, A.; Tolazzi, M.; Sanadar, M.; Melchior, A. Hydrometallurgical Recovery of Metals from Spent Lithium-Ion Batteries with Ionic Liquids and Deep Eutectic Solvents. *J. Environ. Chem. Eng.* **2024**, *12*, 113248. [CrossRef]
40. Sarıkaya, M.; Genceli Güner, F.E.; Benli, B. Deep Eutectic Solvents for Sustainable Recovery of Critical and Rare Metals from Primary and Secondary Resources: A Review. *Physicochem. Probl. Miner. Process.* **2026**, *62*, 224969. [CrossRef]
41. Liu, Q.; Li, Y.; Qiu, Y.; Zhang, J.; Cheng, H.; Song, Z.; Qi, Z. Deep Eutectic Solvents for High-Efficiency Recovery of Valuable Metals from Spent Lithium-Ion Batteries: Rational Design and Mechanistic Insights. *Green Chem.* **2025**, *27*, 10735–10754. [CrossRef]
42. Beauchemin, S.; Langley, S.; MacKinnon, T. Geochemical Properties of 40-Year Old Forested Pyrrhotite Tailings and Impact of Organic Acids on Metal Cycling. *Appl. Geochem.* **2019**, *110*, 104437. [CrossRef]
43. Kosson, D.S.; Van Der Sloot, H.A.; Sanchez, F.; Garrabrants, A.C. An Integrated Framework for Evaluating Leaching in Waste Management and Utilization of Secondary Materials. *Environ. Eng. Sci.* **2002**, *19*, 159–204. [CrossRef]
44. Van Herck, P.; Vandecasteele, C. Evaluation of the Use of a Sequential Extraction Procedure for the Characterization and Treatment of Metal Containing Solid Waste. *Waste Manag.* **2001**, *21*, 685–694. [CrossRef]
45. Xu, X.; Zhou, S.; Li, B.; Wei, Y.; Wang, H. Investigation Interfacial Wetting Behavior of Copper Matte/Slag/Fe3O4 Enriched Intermediate Layer during High Temperature Smelting. *Metall. Mater. Trans. B* **2025**, *56*, 449–471. [CrossRef]
46. Chen, Z.; Wei, D.; Ma, Y.; Shi, Y.; Chen, J. Experimental Investigation and Thermodynamic Optimization of the Fe–Ta–W System. *Intermetallics* **2026**, *198*, 109559. [CrossRef]
47. Cheng, X.; Zhu, Z.; Hai, R.; Hui, C.; Guo, S. Meso-Structure Study of Recycled Aggregate Stabilized by Multi-Source Solid Waste Geopolymer Based on Discrete Element Method. *AIP Adv.* **2026**, *16*, 095205. [CrossRef]
48. Haberl, J.; Schuster, M. Solubility of Elements in Waste Incineration Fly Ash and Bottom Ash under Various Leaching Conditions Studied by a Sequential Extraction Procedure. *Waste Manag.* **2019**, *87*, 268–278. [CrossRef]
49. Tian, Y.; Wang, R.; Luo, Z.; Wang, R.; Yang, F.; Wang, Z.; Shu, J.; Chen, M. Heavy Metals Removing from Municipal Solid Waste Incineration Fly Ashes by Electric Field-Enhanced Washing. *Materials* **2020**, *13*, 793. [CrossRef]
50. Barik, S.P.; Park, K.-H.; Parhi, P.K.; Park, J.T. Direct Leaching of Molybdenum and Cobalt from Spent Hydrodesulphurization Catalyst with Sulphuric Acid. *Hydrometallurgy* **2012**, *111–112*, 46–51. [CrossRef]
51. Jamieson, H.E.; Walker, S.R.; Parsons, M.B. Mineralogical Characterization of Mine Waste. *Appl. Geochem.* **2015**, *57*, 85–105. [CrossRef]
52. Guo, H.; Chen, K.; Wang, J.; Gafurovich, K.; Raimovna, K.; Mao, L. Recycling of Li and Transition Metals from Spent Lithium-Ion Batteries Cathodes by Sequential Formic Acid and Deep Eutectic Solvent Leaching. *J. Ind. Eng. Chem.* **2026**, *158*, 242–254. [CrossRef]
53. Jenkin, G.R.T.; Al-Bassam, A.Z.M.; Harris, R.C.; Abbott, A.P.; Smith, D.J.; Holwell, D.A.; Chapman, R.J.; Stanley, C.J. The Application of Deep Eutectic Solvent Ionic Liquids for Environmentally-Friendly Dissolution and Recovery of Precious Metals. *Miner. Eng.* **2016**, *87*, 18–24. [CrossRef]
54. Knight, M.; Van Wyk, P.; Akdogan, G.; Bradshaw, S. Leaching Platinum Group Metals from Simulated Spent Auto-Catalyst Material Using Ozone and Hydrochloric Acid. *Minerals* **2024**, *14*, 998. [CrossRef]
55. Villemejeanne, B.; Legeai, S.; Meux, E.; Dourdain, S.; Mendil-Jakani, H.; Billy, E. ElectroLeaching-ElectroChemical Deposition (EL-ECD) of Gold and Palladium in a Deep Eutectic Solvent (DES). *J. Environ. Chem. Eng.* **2022**, *10*, 108004. [CrossRef]
56. Xv, B.; Li, Z.; Zha, G.; Liu, D.; Yang, B.; Jiang, W. Recovery of Platinum Group Metals from Spent Automotive Catalysts: Review of Conventional Techniques and Vacuum Metallurgy. *Resour. Conserv. Recycl.* **2025**, *215*, 108103. [CrossRef]
57. Ding, Y.; Zheng, H.; Li, J.; Zhang, S.; Liu, B.; Ekberg, C. An Efficient Leaching of Palladium from Spent Catalysts through Oxidation with Fe(III). *Materials* **2019**, *12*, 1205. [CrossRef]
58. Pan, J.; Zhou, C.; Liu, C.; Tang, M.; Cao, S.; Hu, T.; Ji, W.; Luo, Y.; Wen, M.; Zhang, N. Modes of Occurrence of Rare Earth Elements in Coal Fly Ash: A Case Study. *Energy Fuels* **2018**, *32*, 9738–9743. [CrossRef]
59. Li, M.; Ihli, J.; Verheijen, M.A.; Holler, M.; Guizar-Sicairos, M.; Van Bokhoven, J.A.; Hensen, E.J.M.; Weber, T. Alumina-Supported NiMo Hydrotreating Catalysts–aspects of 3D Structure, Synthesis, and Activity. *J. Phys. Chem. C* **2022**, *126*, 18536–18549. [CrossRef]
60. Akcil, A.; Vegliò, F.; Ferella, F.; Okudan, M.D.; Tuncuk, A. A Review of Metal Recovery from Spent Petroleum Catalysts and Ash. *Waste Manag.* **2015**, *45*, 420–433. [CrossRef]
61. Louwers, S.P.A.; Prins, R. Ni EXAFS Studies of the Ni–Mo–S Structure in Carbon-Supported and Alumina-Supported Ni–Mo Catalysts. *J. Catal.* **1992**, *133*, 94–111. [CrossRef]
62. Jafari, M.; Shafaie, S.Z.; Abdollahi, H.; Entezari-Zarandi, A. A Green Approach for Selective Ionometallurgical Separation of Lithium from Spent Li-Ion Batteries by Deep Eutectic Solvent (DES): Process Optimization and Kinetics Modeling. *Miner. Process. Extr. Metall. Rev.* **2023**, *44*, 218–230. [CrossRef]
63. Manthiram, A. A Reflection on Lithium-Ion Battery Cathode Chemistry. *Nat. Commun.* **2020**, *11*, 1550. [CrossRef]

64. He, J.; Song, T.; Zhu, L.; Guo, S.; Yang, B.; Gong, W. Effective Enrichment of REEs from Coal-Series Kaolin by Combining Ammonium Salt Roasting with Eco-Friendly Deep Eutectic Solvents. *Sep. Purif. Technol.* **2026**, *384*, 136259. [CrossRef]
65. Wang, X.; Cheng, W.; Yang, R.; Zang, J. Characterization and Acid Leaching of Rare Earth Elements in Coal Gangue Using Pretreatment of Selective Grinding, Tailings Discarding and Alkali Roasting. *J. Rare Earths* **2025**, *43*, 384–396. [CrossRef]
66. Drogobuzhskaya, S.; Frolova, M.; Shishov, A.; Tsvetov, N. Comparison of Extraction Abilities of Deep Eutectic Solvents and Aqueous Acid Solutions for Extraction of Rare Earths and Transition Metals. *J. Rare Earths* **2024**, *42*, 1157–1164. [CrossRef]
67. Aragón-Tobar, C.F.; Endara, D.; De La Torre, E. Dissolution of Metals (Cu, Fe, Pb, and Zn) from Different Metal-Bearing Species (Sulfides, Oxides, and Sulfates) Using Three Deep Eutectic Solvents Based on Choline Chloride. *Molecules* **2024**, *29*, 290. [CrossRef]
68. Yan, Q.; Ding, A.; Li, M.; Liu, C.; Xiao, C. Green Leaching of Lithium-Ion Battery Cathodes by Ascorbic Acid Modified Guanidine-Based Deep Eutectic Solvents. *Energy Fuels* **2023**, *37*, 1216–1224. [CrossRef]
69. Li, B.; Li, C.; Wang, J.; Wan, R.; Chen, J.; Liu, Y.; Zhang, Z.; Bin, Y.; Yang, X.; Bao, C.; et al. High-Efficiency Leaching of Valuable Metals from Waste Lithium-Ion Ternary Batteries under Mild Conditions Using Green Deep Eutectic Solvents. *Green Chem.* **2025**, *27*, 163–178. [CrossRef]
70. Su, R.; Tang, S.; Wang, Y.; Zhang, M.; Guo, M. Ethanol-Driven Bifunctional Deep Eutectic Solvents for Efficient in Situ Selective Recovery of Valuable Metals from Spent Lithium Batteries. *Sep. Purif. Technol.* **2025**, *364*, 132577. [CrossRef]
71. He, X.; Wen, Y.; Wang, X.; Cui, Y.; Li, L.; Ma, H. Leaching NCM Cathode Materials of Spent Lithium-Ion Batteries with Phosphate Acid-Based Deep Eutectic Solvent. *Waste Manag.* **2023**, *157*, 8–16. [CrossRef]
72. Cheng, M.; Hua, Y.; Zhang, Q.; Li, Q.; Li, H.; Wang, D.; Wang, X.; Zhao, Y.; Ru, J.; Li, B. H2O-Balance-Regulated Cation–Anion Competitive Coordination for Selective Elements Extraction from Spent Lithium-Ion Batteries. *eScience* **2024**, *4*, 100275. [CrossRef]
73. Wang, C.; Ai, T.; Gao, X.; Lu, J.; Liu, J.; Zhu, W.; Luo, Y. Effective Recycling of Critical Metals from LiCoO2 Batteries by Hydrated Deep Eutectic Solvents: Performance, Kinetic and Mechanism. *J. Water Process Eng.* **2024**, *59*, 105088. [CrossRef]
74. Chen, J.; Sun, S.; Luo, X.; Xiao, F.; Chen, J.; Yang, Z.; Sui, C.; Yu, K.; Tu, G. Highly Selective Recovery of Valuable Metals from Spent Hydrotreating Catalysts via Deep Eutectic Solvents. *J. Environ. Chem. Eng.* **2025**, *13*, 117123. [CrossRef]
75. Wang, Z.; Liu, M.; Gao, B.; Mao, L. Selective Leaching and Stepwise Separation of V, Mo, and Ni from Spent HDS Catalysts Using a Green Deep Eutectic Solvent. *J. Environ. Chem. Eng.* **2026**, *14*, 123212. [CrossRef]
76. Ebrahimi, E.; Abdollahi, H.; Shafaei, S.; Ghanbarzad, M.; Talebi, E. Green Extraction of Pure Ferromagnetic Nickel from Spent Hydroprocessing Catalysts via Deep Eutectic Solvents. *Sep. Purif. Technol.* **2023**, *313*, 123461. [CrossRef]
77. Heo, S.; Kim, R.; Yoon, H.-S.; Kim, C.-J.; Chung, K.W.; Lee, S. Effect of Pretreatment Methods on the Selective Leaching of Rare Earth Elements from NdFeB Permanent Magnets Using Deep Eutectic Solvents. *Hydrometallurgy* **2024**, *226*, 106284. [CrossRef]
78. Topçu, M.A.; Rüşen, A.; Küçük, Ö. Treatment of Copper Converter Slag with Deep Eutectic Solvent as Green Chemical. *Waste Manag.* **2021**, *132*, 64–73. [CrossRef]
79. Zhu, X.; Xu, C.; Tang, J.; Hua, Y.; Zhang, Q.; Liu, H.; Wang, X.; Huang, M. Selective Recovery of Zinc from Zinc Oxide Dust Using Choline Chloride Based Deep Eutectic Solvents. *Trans. Nonferrous Met. Soc. China* **2019**, *29*, 2222–2228. [CrossRef]
80. Wang, S.; Xu, C.; Lei, Z.; Li, J.; Lu, J.; Xiang, Q.; Chen, X.; Hua, Y.; Li, Y. Recycling of Zinc Oxide Dust Using ChCl-Urea Deep Eutectic Solvent with Nitrilotriacetic Acid as Complexing Agents. *Miner. Eng.* **2022**, *175*, 107295. [CrossRef]
81. Rodriguez, N.; Machiels, L.; Onghena, B.; Spooren, J.; Binnemans, K. Selective Recovery of Zinc from Goethite Residue in the Zinc Industry Using Deep-Eutectic Solvents. *RSC Adv.* **2020**, *10*, 7328–7335. [CrossRef]
82. Sarker, S.K.; Yadav, S.; Haque, N.; Pramanik, B.K. Impact of Alkali Roasting and Leaching Conditions on the Recovery of Rare Earth Elements from Iron-Rich Mine Tailings: A Study Using Deep Eutectic Solvents. *Process Saf. Environ. Prot.* **2025**, *199*, 107259. [CrossRef]
83. Damilano, G.; Laitinen, A.; Willberg-Keyriläinen, P.; Lavonen, T.; Häkkinen, R.; Dehaen, W.; Binnemans, K.; Kuutti, L. Effects of Thiol Substitution in Deep-Eutectic Solvents (DESs) as Solvents for Metal Oxides. *RSC Adv.* **2020**, *10*, 23484–23490. [CrossRef]
84. Güloğlu, E.; Yardimci, H.A.; Ilhan, S.; Kalpakli, A.O.; Zoraga, M.; Orhan, G. Leaching Kinetics and Selective Recovery of Co, Mo, and al from Spent Co-Mo Hydrodesulfurization Catalyst in Choline Chloride:P-Toluene Sulfonic Acid Media. *Hydrometallurgy* **2026**, *243*, 106762. [CrossRef]
85. Wen, Y.; He, X.; Di, S.; Liu, K.; Li, D.; Du, J. Comparative of Malonic Acid Aqueous Solution and Malonic Acid-Based Deep Eutectic Solvent for $LiCoO_2$ Cathode Materials Recovery: Leaching Efficiency and Mechanism. *J. Environ. Chem. Eng.* **2023**, *11*, 110979. [CrossRef]
86. Zhang, Y.; Cui, P.; Luo, G.; Chen, L.; Li, X.; Chao, Y.; Zhu, W. One-Step Selective Separation and Efficient Recovery of Valuable Metals from Spent Lithium Batteries by Phosphoric Acid-Based Deep Eutectic Solvent. *Green Chem. Eng.* **2024**, *5*, 390–398. [CrossRef]
87. Yetim, D.; Svecova, L.; Leprêtre, J.-C. Lithium-Ion Battery Cathode Recycling through a Closed-Loop Process Using a Choline Chloride-Ethylene Glycol-Based Deep-Eutectic Solvent in the Presence of Acid. *ChemistryOpen* **2024**, *13*, e202300061. [CrossRef]
88. Valverde, I.M.; Paulino, J.F.; Afonso, J.C. Hydrometallurgical Route to Recover Molybdenum, Nickel, Cobalt and Aluminum from Spent Hydrotreating Catalysts in Sulphuric Acid Medium. *J. Hazard. Mater.* **2008**, *160*, 310–317. [CrossRef]

89. Or, T.; Gourley, S.W.D.; Kaliyappan, K.; Yu, A.; Chen, Z. Recycling of Mixed Cathode Lithium-Ion Batteries for Electric Vehicles: Current Status and Future Outlook. *Carbon Energy* **2020**, *2*, 6–43. [CrossRef]
90. Oke, E.A.; Potgieter, J.H. Effectiveness of Acidic Deep Eutectic Solvents in Recovery of Hazardous Base Metals from Waste Printed Circuit Boards. *Environ. Sci. Pollut. Res.* **2025**, *32*, 16361–16379. [CrossRef]
91. Yang, P.; Zhou, L.; Zeng, J.; Ye, Y.; Lan, J.; Xie, X.; Chen, Y.; Wang, X.; Ao, R. Sustainable Recovery of Cobalt and Lithium from Spent Lithium-Ion Batteries Using Water-Based Deep Eutectic Solvents. *J. Environ. Chem. Eng.* **2026**, *14*, 120726. [CrossRef]
92. Zhu, J.; Chen, W.; Shi, W.; Lu, G.; Jia, W.; Wan, Q.; Yu, Q.; Chen, Z. Synergistic Promotion by Acidity and Reducibility for the Mild and Efficient Leaching of Lithium Cobalt Oxide in Deep Eutectic Solvents: Mechanism Elucidation. *ACS Sustain. Chem. Eng.* **2025**, *13*, 19858–19870. [CrossRef]
93. Bidari, E.; Winardhi, C.W.; Godinho, J.R.D.A.; Frisch, G. Role of Oxidants in Metal Extraction from Sulfide Minerals in a Deep Eutectic Solvent. *ACS Omega* **2024**, *9*, 14592–14603. [CrossRef]
94. Hartley, J.M.; Scott, S.; Dilruba, Z.; Lucio, A.J.; Bird, P.J.; Harris, R.C.; Jenkin, G.R.T.; Abbott, A.P. Iodine Speciation in Deep Eutectic Solvents. *Phys. Chem. Chem. Phys.* **2022**, *24*, 24105–24115. [CrossRef]
95. Moreno, K.; Díaz, X.; Endara, D.; Sánchez, F.; Aragón-Tobar, C.F. Zinc and Lead Leaching from Sphalerite–Galena Concentrate Using Deep Eutectic Solvents Based on Choline Chloride: Effect of Roasting and Iodine as Oxidizing Agent. *Molecules* **2024**, *29*, 3742. [CrossRef]
96. Feng, F.; Wang, M.; Zhang, J.; Ding, H.; Yu, L.; Guo, W.; Guo, L.; Liang, Q.; Zhang, Q.; Lu, C.; et al. Hydrogen Bonding-Based Deep Eutectic Solvents for Choline Chloride/Sulfamide and Its Application in the Recycling of Precious Metals. *J. Environ. Chem. Eng.* **2024**, *12*, 113611. [CrossRef]
97. Meles Neguse, S.; Yoon, S.; Lim, H.; Jang, J.; Baek, S.; Jöckel, D.M.; Widenmeyer, M.; Balke-Grünewald, B.; Weidenkaff, A. The Pitfalls of Deep Eutectic Solvents in the Recycling of Lithium-Ion Batteries. *Energy Technol.* **2024**, *12*, 2301213. [CrossRef]
98. Chen, Y.; Luo, S.; Liu, P.; Chen, M.; Oluseyi, A.; Zhang, C.; Gao, B.; Huo, K. A Dual Closed-Loop Process to Recycle High Nickel Cathode of Spent Lithium-Ion Batteries via Deep Eutectic Solvents: Computational Screening and Experimental Validation. *Rare Met.* **2026**, *45*, e70003. [CrossRef]
99. Couturier, J.; Levard, C.; Collin, B.; Chaurand, P.; Vidal, V.; Mathon, O.; Duvivier, A.; Angeletti, B.; Borschneck, D.; Rose, J.; et al. Dissolution of Rare Earth Elements: Exploring the Ability of Deep Eutectic Solvents and Organic Acid Solutions, the Case of Lactic Acid. *Sep. Purif. Technol.* **2025**, *366*, 132740. [CrossRef]
100. Perera, I.N.; Dobhal, G.S.; Pringle, J.M.; O'Dell, L.A.; Tawfik, S.A.; Walsh, T.R.; Pozo-Gonzalo, C. A Case Study Using Spectroscopy and Computational Modelling for Co Speciation in a Deep Eutectic Solvent. *Phys. Chem. Chem. Phys.* **2024**, *26*, 21087–21098. [CrossRef]
101. Iname, A.; Vitry, V.; Tapsoba, I. Chemical Speciation of Co^{2+} and Ni^{2+} Ions in Deep Eutectic Solvents and Highly Efficient Colorimetric Determination of Cobalt from Lithium-Ion Battery Samples Using UV/Vis. *J. Mol. Liq.* **2026**, *458*, 129750. [CrossRef]
102. Liu, J.; Liu, Y.; Sui, L.; Zhang, S.; Liu, J. Sustainable and Selective Recovery of Valuable Metals from Spent Catalysts by Green Deep Eutectic Solvents. *J. Environ. Chem. Eng.* **2026**, *14*, 121890. [CrossRef]
103. Chikineva, T.Y.; Zinov'eva, I.V.; Yakovleva, S.A.; Zakhodyaeva, Y.A.; Voshkin, A.A. New Eutectic Solvent Based on Bis(2,4,4-Trimethylpentyl)Phosphinic Acid, Tributyl Phosphate and Phenol for the Extraction of Trivalent Rare-Earth Elements from Nitrate Solutions. *Processes* **2025**, *13*, 2830. [CrossRef]
104. Zinov'eva, I.V.; Chikineva, T.Y.; Zakhodyaeva, Y.A.; Voshkin, A.A. Bis(2,4,4-Trimethylpentyl)Phosphinic Acid/Phenol Deep Eutectic Solvent: Physicochemical Properties and Application Prospects for the Extraction of Trivalent Rare Earth Elements. *J. Mol. Liq.* **2025**, *423*, 126984. [CrossRef]
105. Zhang, Z.; Li, G.; Wang, Z.; Xiao, W.; Lin, Y.; Cheng, S.; Min, R.; Wu, J.; Liu, M.; Wang, D. Encoding Intrinsic Rare-Earth Dissolution Selectivity into Deep Eutectic Solvents via Coordination-Active Functional Group Design. *J. Clean. Prod.* **2026**, *553*, 147995. [CrossRef]
106. Tang, N.; Liu, L.; Yin, C.; Zhu, G.; Huang, Q.; Dong, J.; Yang, X.; Wang, S. Environmentally Benign Hydrophobic Deep Eutectic Solvents for Palladium(II) Extraction from Hydrochloric Acid Solution. *J. Taiwan Inst. Chem. Eng.* **2021**, *121*, 92–100. [CrossRef]
107. Matzapetakis, M.; Dakanali, M.; Raptopoulou, C.P.; Tangoulis, V.; Terzis, A.; Moon, N.; Giapintzakis, J.; Salifoglou, A. Synthesis, Spectroscopic, and Structural Characterization of the First Aqueous Cobalt(II)-Citrate Complex: Toward a Potentially Bioavailable Form of Cobalt in Biologically Relevant Fluids. *J. Biol. Inorg. Chem.* **2000**, *5*, 469–474. [CrossRef]
108. Hammond, O.S.; Bathke, E.K.; Bowron, D.T.; Edler, K.J. Trace Water Changes Metal Ion Speciation in Deep Eutectic Solvents: Ce^{3+} Solvation and Nanoscale Water Clustering in Choline Chloride–Urea–Water Mixtures. *Inorg. Chem.* **2023**, *62*, 18069–18078. [CrossRef]
109. Deng, H.; Xu, J.; Yang, G.; Shi, Z.; Zhu, H.; He, W.; Li, G. Inactive Diluent-Modified Deep Eutectic Solvents for Highly Selective Extraction of Transition Metals from Waste Lithium-Ion Batteries: Molecular Insights and Process Investigation. *J. Colloid Interface Sci.* **2026**, *724*, 141184. [CrossRef]

110. Binnemans, K.; Jones, P.T. Ionic Liquids and Deep-Eutectic Solvents in Extractive Metallurgy: Mismatch between Academic Research and Industrial Applicability. *J. Sustain. Metall.* **2023**, *9*, 423–438. [CrossRef]
111. Yadav, J.; Sarker, S.K.; Bruckard, W.; Jegatheesan, V.; Haque, N.; Pramanik, B.K. Selective Recovery of Rare Earth Elements from NdFeB Magnet Waste via Deep Eutectic Solvents: Process Optimization and DFT Insights. *Sep. Purif. Technol.* **2025**, *376*, 134176. [CrossRef]
112. Abbott, A.P.; Boothby, D.; Capper, G.; Davies, D.L.; Rasheed, R.K. Deep Eutectic Solvents Formed between Choline Chloride and Carboxylic Acids: Versatile Alternatives to Ionic Liquids. *J. Am. Chem. Soc.* **2004**, *126*, 9142–9147. [CrossRef]
113. Pateli, I.M.; Thompson, D.; Alabdullah, S.S.M.; Abbott, A.P.; Jenkin, G.R.T.; Hartley, J.M. The Effect of pH and Hydrogen Bond Donor on the Dissolution of Metal Oxides in Deep Eutectic Solvents. *Green Chem.* **2020**, *22*, 5476–5486. [CrossRef]
114. Alhashim, S.H.; Bhattacharyya, S.; Tromer, R.; Kabbani, A.; Babu, G.; Oliveira, E.F.; Galvao, D.S.; Ajayan, P.M. Mechanistic Study of Lithium-Ion Battery Cathode Recycling Using Deep Eutectic Solvents. *ACS Sustain. Chem. Eng.* **2023**, *11*, 6914–6922. [CrossRef]
115. Cheng, Q.; Zhao, X.; Yang, G.; Mao, L.; Liao, F.; Chen, L.; He, P.; Pan, D.; Chen, S. Recent Advances of Metal Phosphates-Based Electrodes for High-Performance Metal Ion Batteries. *Energy Storage Mater.* **2021**, *41*, 842–882. [CrossRef]
116. Kolker, A.; Scott, C.; Hower, J.C.; Vazquez, J.A.; Lopano, C.L.; Dai, S. Distribution of Rare Earth Elements in Coal Combustion Fly Ash, Determined by SHRIMP-RG Ion Microprobe. *Int. J. Coal Geol.* **2017**, *184*, 1–10. [CrossRef]
117. Liu, P.; Huang, R.; Tang, Y. Comprehensive Understandings of Rare Earth Element (REE) Speciation in Coal Fly Ashes and Implication for REE Extractability. *Environ. Sci. Technol.* **2019**, *53*, 5369–5377. [CrossRef]
118. Pateli, I.M.; Abbott, A.P.; Jenkin, G.R.T.; Hartley, J.M. Electrochemical Oxidation as Alternative for Dissolution of Metal Oxides in Deep Eutectic Solvents. *Green Chem.* **2020**, *22*, 8360–8368. [CrossRef]
119. Rimsza, J.M.; Corrales, L.R. Adsorption Complexes of Copper and Copper Oxide in the Deep Eutectic Solvent 2:1 Urea–Choline Chloride. *Comput. Theor. Chem.* **2012**, *987*, 57–61. [CrossRef]
120. Liu, K.; Zhang, Y.; Wang, M.; Zhu, X.; Maboudian, R.; Tsang, D.C.W. Dissolution of Spent Lithium-ion Battery Cathode Materials: Overlooked Significance of Aluminum Impurities. *Adv. Sci.* **2025**, *12*, 2417737. [CrossRef]
121. Chang, X.; Fan, M.; Gu, C.; He, W.; Meng, Q.; Wan, L.; Guo, Y. Selective Extraction of Transition Metals from Spent $LiNi_xCo_yMn_{1-x-y}O_2$ Cathode via Regulation of Coordination Environment. *Angew. Chem. Int. Ed.* **2022**, *61*, e202202558. [CrossRef]
122. Velez, C.; Acevedo, O. Simulation of Deep Eutectic Solvents: Progress to Promises. *WIREs Comput. Mol. Sci.* **2022**, *12*, e1598. [CrossRef]
123. Lyu, Y.; Yuwono, J.; Fan, Y.; Li, J.; Wang, J.; Zeng, R.; Davey, K.; Mao, J.; Zhang, C.; Guo, Z. Selective Extraction of Critical Metals from Spent Li-Ion Battery Cathode: Cation-Anion Coordination and Anti-Solvent Crystallization. *Adv. Mater.* **2024**, *36*, 2312551. [CrossRef]
124. De Villiers Engelbrecht, L.; Cibotariu, N.; Ji, X.; Laaksonen, A.; Mocci, F. Deep Eutectic Solvents Meet Non-Aqueous Cosolvents: A Modeling and Simulation Perspective—A Tutorial Review. *J. Chem. Eng. Data* **2025**, *70*, 19–43. [CrossRef]
125. Ma, C.; Laaksonen, A.; Liu, C.; Lu, X.; Ji, X. The Peculiar Effect of Water on Ionic Liquids and Deep Eutectic Solvents. *Chem. Soc. Rev.* **2018**, *47*, 8685–8720. [CrossRef]
126. Abranches, D.O.; Coutinho, J.A.P. Everything You Wanted to Know about Deep Eutectic Solvents but Were Afraid to Be Told. *Annu. Rev. Chem. Biomol. Eng.* **2023**, *14*, 141–163. [CrossRef]
127. Gholami, S.; Pérez-Page, M.; D'Agostino, C.; Esteban, J. (Deep) Eutectic Solvents for the Separation of Platinum Group Metals and Rare Earth Elements: Characteristics, Extraction Mechanisms and State of the Art. *Chem. Eng. J.* **2025**, *505*, 159497. [CrossRef]
128. Lustig, S.R. Speciation in Electrolytes Using the COSMO-RS Solution Model. *Fluid Phase Equilib.* **2020**, *521*, 112717. [CrossRef]
129. Yuan, Z.; Liu, H.; Yong, W.F.; She, Q.; Esteban, J. Status and Advances of Deep Eutectic Solvents for Metal Separation and Recovery. *Green Chem.* **2022**, *24*, 1895–1929. [CrossRef]
130. Song, Z.; Wang, J.; Sundmacher, K. Evaluation of COSMO-RS for Solid–Liquid Equilibria Prediction of Binary Eutectic Solvent Systems. *Green Energy Environ.* **2021**, *6*, 371–379. [CrossRef]
131. Bernicot, B.; Arrachart, G.; Dourdain, S.; Schaeffer, N.; Teixeira, G.; Pellet-Rostaing, S. Design and Characterization of Novel Hydrophobic Eutectic Solvents Based on Metal-Extracting Ligands. *J. Mol. Liq.* **2025**, *427*, 127332. [CrossRef]
132. Farias, F.O.; Pereira, J.F.B.; Coutinho, J.A.P.; Igarashi-Mafra, L.; Mafra, M.R. Understanding the Role of the Hydrogen Bond Donor of the Deep Eutectic Solvents in the Formation of the Aqueous Biphasic Systems. *Fluid Phase Equilib.* **2020**, *503*, 112319. [CrossRef]
133. Amusa, H.K.; Lemaoui, T.; Almustafa, G.; Darwish, A.S.; Banat, F.; Arafat, H.A.; AlNashef, I.M. Advancing Circular Battery Recycling by Systematically Screening Novel Deep Eutectic Solvents for Sustainable Metal Recovery. *Sustain. Mater. Technol.* **2025**, *44*, e01383. [CrossRef]
134. Guidugli, L.F.; Reza, T. Extraction of Rare Earth Elements from Water by Trioctylphosphine Oxide-Based Hydrophobic Deep Eutectic Solvents. *Ind. Eng. Chem. Res.* **2024**, *63*, 12582–12590. [CrossRef]
135. Cheng, M.; Ru, J.; Zhang, Q.; Hua, Y.; Xu, C.; Zhang, Y.; Wang, D. One-Step Direct Recovery of Lithium from Spent Lithium-Ion Batteries via Water-Based Deep Eutectic Solvent. *ACS Sustain. Chem. Eng.* **2025**, *13*, 1719–1728. [CrossRef]

136. Hammond, O.S.; Bowron, D.T.; Edler, K.J. The Effect of Water upon Deep Eutectic Solvent Nanostructure: An Unusual Transition from Ionic Mixture to Aqueous Solution. *Angew. Chem. Int. Ed.* **2017**, *56*, 9782–9785. [CrossRef]
137. Sapir, L.; Harries, D. Restructuring a Deep Eutectic Solvent by Water: The Nanostructure of Hydrated Choline Chloride/Urea. *J. Chem. Theory Comput.* **2020**, *16*, 3335–3342. [CrossRef]
138. Tian, Y.; Zhang, H.; Qiao, Y.; Yang, H.; Liu, Y.; Ji, X. Intelligent Prediction of Ionic Liquids and Deep Eutectic Solvents by Machine Learning. *Chin. J. Chem. Eng.* **2025**, *84*, 227–243. [CrossRef]
139. Scheffczyk, J.; Fleitmann, L.; Schwarz, A.; Lampe, M.; Bardow, A.; Leonhard, K. COSMO-CAMD: A Framework for Optimization-Based Computer-Aided Molecular Design Using COSMO-RS. *Chem. Eng. Sci.* **2017**, *159*, 84–92. [CrossRef]
140. Amusa, H.K.; Lemaoui, T.; Almustafa, G.; Darwish, A.S.; Banat, F.; Arafat, H.A.; AlNashef, I.M. Synergistic Ternary Deep Eutectic Solvents: An Archetype for Sustainable and Eco-Conscious Li and Co Recovery from Spent Batteries. *Chem. Eng. J.* **2024**, *499*, 156114. [CrossRef]
141. Nurfajrin, Z.D.; Fajar, A.T.N.; Maghfirah, A.; Goto, M. Accelerated Screening of Deep Eutectic Solvents for Nickel/Cobalt Extraction: Integrating Quantum Chemistry, Machine Learning, and Experimental Validation. *Ind. Eng. Chem. Res.* **2025**, *64*, 6655–6663. [CrossRef]
142. Zhu, J.; Jin, J.; Ju, L.; Xia, Y.; Zou, Y.; Yang, H.; Xu, R. WSO–SVM-Based Optimization of Low-Carbon Composite Flocculant and Its Microstructural Mechanism for Engineering Waste Slurry Dewatering. *Can. Geotech. J.* **2026**, *63*, 1–25. [CrossRef]
143. Artrith, N.; Butler, K.T.; Coudert, F.-X.; Han, S.; Isayev, O.; Jain, A.; Walsh, A. Best Practices in Machine Learning for Chemistry. *Nat. Chem.* **2021**, *13*, 505–508. [CrossRef]
144. Janet, J.P.; Duan, C.; Yang, T.; Nandy, A.; Kulik, H.J. A Quantitative Uncertainty Metric Controls Error in Neural Network-Driven Chemical Discovery. *Chem. Sci.* **2019**, *10*, 7913–7922. [CrossRef]
145. Rodrigues, T. The Good, the Bad, and the Ugly in Chemical and Biological Data for Machine Learning. *Drug Discov. Today Technol.* **2019**, *32–33*, 3–8. [CrossRef]
146. Jin, D.; He, H.; Sun, L.; Zeng, Z.; Liu, Z. An Integrated ML Model for the Prediction of the Melting Points, Phase Diagrams, and Eutectic Points of the Type III and V Deep Eutectic Solvents. *Chem. Eng. Sci.* **2025**, *306*, 121245. [CrossRef]
147. Lemaoui, T.; Darwish, A.S.; Hammoudi, N.E.H.; Abu Hatab, F.; Attoui, A.; Alnashef, I.M.; Benguerba, Y. Prediction of Electrical Conductivity of Deep Eutectic Solvents Using COSMO-RS Sigma Profiles as Molecular Descriptors: A Quantitative Structure–Property Relationship Study. *Ind. Eng. Chem. Res.* **2020**, *59*, 13343–13354. [CrossRef]
148. Gao, W.; Zhu, X.; Hu, C.; Li, G.; Cao, Z.; Yan, S.; Zhou, W. High Solid-to-Liquid Ratio Leaching of Strategic Metals from Spent Lithium-Ion Batteries: Design of a Green and Sustainable Deep Eutectic Solvent System. *Green Chem.* **2026**, *28*, 11564–11576. [CrossRef]
149. Xu, M.; Wang, J.; Wang, S.; Zhang, W.; Mao, L.; Gao, B. Stepwise Recycling Valuable Metals from Spent Lithium-Ion Batteries Cathode: High-Efficient Leaching by Deep Eutectic Solvent and Selective Separation by Recrystallization and Electrostatic Interaction. *Sep. Purif. Technol.* **2025**, *376*, 134020. [CrossRef]
150. Li, H.; Chen, N.; Liu, W.; Feng, H.; Su, J.; Fu, D.; Liu, X.; Qiu, M.; Wang, L. A Reusable Deep Eutectic Solvent for the Regeneration of Li and Co Metals from Spent Lithium-Ion Batteries. *J. Alloys Compd.* **2023**, *966*, 171517. [CrossRef]
151. Choi, S.; Motobayashi, K.; Kim, K. Highly Selective and Near-Complete Electrochemical Recovery of Cobalt and Nickel from Spent Batteries through Multifunctional Deep Eutectic Solvent. *Energy Storage Mater.* **2025**, *82*, 104646. [CrossRef]
152. Cheng, J.; Zheng, C.; Xu, K.; Zhu, Y.; Song, Y.; Jing, C. Sequential Separation of Critical Metals from Lithium-Ion Batteries Based on Deep Eutectic Solvent and Electrodeposition. *J. Hazard. Mater.* **2024**, *465*, 133157. [CrossRef]
153. Ma, C.; Gamarra, J.D.; Younesi, R.; Forsberg, K.; Svärd, M. Antisolvent Crystallization from Deep Eutectic Solvent Leachates of $LiNi_{1/3}Mn_{1/3}Co_{1/3}O_2$ for Recycling and Direct Synthesis of Battery Cathodes. *Resour. Conserv. Recycl.* **2023**, *198*, 107210. [CrossRef]
154. Ma, C.; Svärd, M.; Forsberg, K. Recycling Cathode Material $LiCo_{1/3}Ni_{1/3}Mn_{1/3}O_2$ by Leaching with a Deep Eutectic Solvent and Metal Recovery with Antisolvent Crystallization. *Resour. Conserv. Recycl.* **2022**, *186*, 106579. [CrossRef]
155. Wen, Y.; He, X.; Kang, T.; Gu, K.; Di, S.; Li, L.; Cui, Y. Simultaneous Separation and Leaching of Cathode Materials from Spent Lithium-Ion Battery Using Ternary Deep Eutectic Solvents. *J. Environ. Chem. Eng.* **2024**, *12*, 114864. [CrossRef]
156. Chen, S.; Su, S.; Huang, Y.; Liu, B.; Sun, H.; Yang, S.; Han, G. Deep Eutectic Solvents for Separation and Purification Applications in Critical Metal Metallurgy: Recent Advances and Perspectives. *Int. J. Miner. Metall. Mater.* **2025**, *32*, 1–19. [CrossRef]
157. Amphlett, J.T.M.; Choi, S. The Effect of Increasing Water Content on Transition Metal Speciation in Deep Eutectic Solvents. *J. Mol. Liq.* **2021**, *332*, 115845. [CrossRef]
158. Dou, A.; Du, Q.; Zhou, M.; Yan, Z.; Bai, Z.; Tian, J.; Su, M.; Zhou, Y.; Liu, Y.; Liu, L. Mechanistic Insights into Deep Eutectic Solvent-Driven Recycling of Black Mass from Spent Lithium Iron Phosphate Batteries. *J. Environ. Chem. Eng.* **2026**, *14*, 123442. [CrossRef]
159. Shi, H.; Zhang, J.; Ou, L. A Comprehensive Review on the Separation and Purification of Valuable Metals from the Leachate of Spent Lithium-Ion Batteries. *Sep. Purif. Technol.* **2025**, *360*, 130847. [CrossRef]

160. Wang, J.; Wang, Y.; Lyu, Y.; Mao, J.; Guo, Z. Stage-Specific Roles of Deep Eutectic Solvents in Recycling of Spent Lithium-Ion Batteries. *Adv. Energy Mater.* **2026**, *16*, e06741. [CrossRef]
161. Carreira, A.R.F.; Nogueira, A.; Crema, A.P.S.; Passos, H.; Schaeffer, N.; Coutinho, J.A.P. Super Concentrated HCl in a Deep Eutectic Solvent as Media for the Integrated Leaching and Separation of Metals from End-of-Life Lithium-Ion Batteries. *Chem. Eng. J.* **2023**, *475*, 146374. [CrossRef]
162. Lanaridi, O.; Platzer, S.; Nischkauer, W.; Limbeck, A.; Schnuerch, M.; Bica-Schroeder, K. A Combined Deep Eutectic Solvent-Ionic Liquid Process for the Extraction and Separation of Platinum Group Metals (Pt, Pd, Rh). *Molecules* **2021**, *26*, 7204. [CrossRef]
163. Varghese, A.T.; Malar, C.G.; Seenuvasan, M.; Jayapradha, V. Neodymium Recovery from Permanent Magnets: A Breakthrough Approach Using Deep Eutectic Solvents and Mica. *J. Mol. Liq.* **2024**, *394*, 123690. [CrossRef]
164. Abbott, A.P.; Harris, R.C.; Holyoak, F.; Frisch, G.; Hartley, J.; Jenkin, G.R.T. Electrocatalytic Recovery of Elements from Complex Mixtures Using Deep Eutectic Solvents. *Green Chem.* **2015**, *17*, 2172–2179. [CrossRef]
165. Wang, J.; Yuwono, J.; Wang, Y.; Lyu, Y.; Liu, S.; Hall, T.; Zeng, R.; Mao, J.; Guo, Z. Selective Lithium Recovery via Stepwise Transition Metal Crystallization in a Natural Deep Eutectic Solvent. *Adv. Sci.* **2025**, *12*, e14509. [CrossRef]
166. Ma, C.; Mohamoud, M.; Punt, T.; Li, J.; Svärd, M.; Forsberg, K. Crystallization of Cathode Active Material Precursors from Tartaric Acid Solution. *ChemSusChem* **2025**, *18*, e202401523. [CrossRef]
167. Zou, J.; Zhang, R.; Huang, Y.; Wang, X.; Chen, L.; Sun, X.; Wang, M.; Zhang, Y.; Wu, K. High Efficiency Leaching of Black Powder from Spent Lithium-Ion Battery by Ternary Deep Eutectic Solvent and Recovery of Metals by Precipitation and Electrodeposition. *Sep. Purif. Technol.* **2025**, *364*, 132438. [CrossRef]
168. Guamán-Gualancañay, J.M.; Aragón-Tobar, C.F.; Moreno, K.; Palacios, J.-L.; Endara, D. Recovery of Lithium and Cobalt from Spent Lithium-Ion Batteries Using a Deep Eutectic Solvent Based on Choline Chloride and Oxalic Acid (Oxaline). *Molecules* **2025**, *30*, 4690. [CrossRef]
169. Martín, M.I.; García-Díaz, I.; López, F.A. Properties and Perspective of Using Deep Eutectic Solvents for Hydrometallurgy Metal Recovery. *Miner. Eng.* **2023**, *203*, 108306. [CrossRef]
170. Yu, L.; Li, Z.; Huang, W.; Ali, A.; Chen, Y.; Zhao, G.; Yao, S. Recovery and Post-Treatment Processes for Ionic Liquids and Deep Eutectic Solvents. *J. Mol. Liq.* **2024**, *402*, 124767. [CrossRef]
171. Abu Hatab, F.; Ibrahim, O.A.Z.; Warrag, S.E.E.; Darwish, A.S.; Lemaoui, T.; Alam, M.M.; Alsufyani, T.; Jevtovic, V.; Jeon, B.-H.; Banat, F.; et al. Solvent Regeneration Methods for Combined Dearomatization, Desulfurization, and Denitrogenation of Fuels Using Deep Eutectic Solvents. *ACS Omega* **2023**, *8*, 626–635. [CrossRef]
172. Tang, Y.; Sun, Z.; Li, A.; Lv, C.; Fu, Z.; Fu, Z. Regeneration of Deep Eutectic Solvents: Technologies, Mechanisms, Applications, and Challenges. *J. Environ. Chem. Eng.* **2026**, *14*, 123842. [CrossRef]
173. Wang, Y.; Goikolea, E.; De Larramendi, I.R.; Lanceros-Méndez, S.; Zhang, Q. Efficient Water-Assisted Precipitation of Nickel, Manganese, and Cobalt from Ethaline Deep Eutectic Solvent. *J. Alloys Compd.* **2026**, *1059*, 187130. [CrossRef]
174. Chai, N.; Nie, Q.; Shi, H.; Cui, Y.; Li, W.; Yang, L.; Cao, H.; Yu, H. Synergistic Acidolysis–Reduction–Precipitation Strategy Driven by Natural Solvents for Direct Recovery of Transition Metals from Spent Batteries. *Green Chem.* **2026**, *28*, 1771–1786. [CrossRef]
175. Schiavi, P.; Altimari, P.; Sturabotti, E.; Marrani, A.; Simonetti, G.; Pagnanelli, F. Decomposition of Deep Eutectic Solvent Aids Metals Extraction in Lithium-Ion Batteries Recycling. *ChemSusChem* **2022**, *15*, e202200966. [CrossRef]
176. Domínguez De María, P.; Kara, S. On the Fate of Deep Eutectic Solvents after Their Use as Reaction Media: The CO_2 Production during Downstream and Ultimate Disposal. *RSC Sustain.* **2024**, *2*, 608–615. [CrossRef]
177. Yang, J.H.; Ooi, A.W.S.; Goodwin, Z.A.H.; Xie, Y.; Ding, J.; Falletta, S.; Park, A.-H.A.; Kozinsky, B. Room-Temperature Decomposition of the Ethaline Deep Eutectic Solvent. *J. Phys. Chem. Lett.* **2025**, *16*, 3039–3046. [CrossRef]
178. González-Rivera, J.; Pelosi, C.; Pulidori, E.; Duce, C.; Tiné, M.R.; Ciancaleoni, G.; Bernazzani, L. Guidelines for a Correct Evaluation of Deep Eutectic Solvents Thermal Stability. *Curr. Res. Green Sustain. Chem.* **2022**, *5*, 100333. [CrossRef]
179. Chen, S.; Zhang, Y.; Cheng, F.; Huang, Y.; Cheng, L.; Guo, H.; Wang, J.; Shi, L.; Yi, Q. Designing Principles of Deep Eutectic Solvents for Sustainable Recycling of Spent Lithium-Ion Batteries. *Appl. Energy* **2025**, *401*, 126723. [CrossRef]
180. *ISO 14044:2006*; Environmental Management—Life Cycle Assessment—Requirements and Guidelines. International Organization for Standardization: Geneva, Switzerland, 2006.
181. Woeste, R.; Drude, E.-S.; Vrucak, D.; Klöckner, K.; Rombach, E.; Letmathe, P.; Friedrich, B. A Techno-Economic Assessment of Two Recycling Processes for Black Mass from End-of-Life Lithium-Ion Batteries. *Appl. Energy* **2024**, *361*, 122921. [CrossRef]
182. Zheng, S.; Xu, S.; Wang, Z.; Duan, H.; Chen, D.; Long, M.; Li, Y. Efficient Leaching of Valuable Metals from Spent Lithium-Ion Batteries Using Green Deep Eutectic Solvents: Process Optimization, Mechanistic Analysis, and Environmental Impact Assessment. *J. Clean. Prod.* **2024**, *480*, 144128. [CrossRef]
183. *IEC 61882:2016*; Hazard and Operability Studies (HAZOP Studies)—Application Guide. International Electrotechnical Commission: Geneva, Switzerland, 2016.

184. Putranto, A.W.; Suhartini, S.; Wibisono, Y.; Masruchin, N.; Chua, A.S.M.; Ngoh, G.C. Life Cycle Assessment of Deep Eutectic Solvent Employment for Sustainable Nanocellulose Production from Biomass: A Systematic Review. *Green Chem. Lett. Rev.* **2025**, *18*, 2507283. [CrossRef]
185. *ISO 14040:2006*; Environmental Management—Life Cycle Assessment—Principles and Framework. International Organization for Standardization: Geneva, Switzerland, 2006.
186. dela-Huerta-Sainz, S.; Diez-Cabanes, V.; Santamaría, S.; Escobedo, M.; Marcos, P.A.; Bol-Arreba, A.; Trenzado, J.L.; Atilhan, M.; Aparicio, S. DES Ecoscale: A Quantitative Sustainability Assessment Framework for Deep Eutectic Solvents. *ACS Sustain. Chem. Eng.* **2026**, *14*, 11573–11590. [CrossRef]
187. Hayyan, M. The Environmental Origin and Fate of Deep Eutectic Solvents: A Two-Edged Sword in Sustainability Claims. *J. Mol. Liq.* **2025**, *439*, 128928. [CrossRef]
188. Wang, M.; Xu, Z.; Dutta, S.; Liu, K.; Labianca, C.; Clark, J.H.; Zimmerman, J.B.; Tsang, D.C.W. Integrated Assessment of Deep Eutectic Solvents Questions Solvometallurgy as a Sustainable Recycling Approach for Lithium-Ion Batteries. *One Earth* **2023**, *6*, 1400–1413. [CrossRef]
189. Ghosh, S.; Ajorloo, M.; Strezov, V. Deep Eutectic Solvents for Circular Waste Valorization: A Review and Future Perspectives Bridging Plastics, Biomass, and e-Waste. *Energy Fuels* **2026**, *40*, 14395–14425. [CrossRef]
190. Cao, Y.; Li, L.; Zhang, Y.; Liu, Z.; Wang, L.; Wu, F.; You, J. Co-Products Recovery Does Not Necessarily Mitigate Environmental and Economic Tradeoffs in Lithium-Ion Battery Recycling. *Resour. Conserv. Recycl.* **2023**, *188*, 106689. [CrossRef]
191. Yoo, E.; Lee, U.; Kelly, J.C.; Wang, M. Life-Cycle Analysis of Battery Metal Recycling with Lithium Recovery from a Spent Lithium-Ion Battery. *Resour. Conserv. Recycl.* **2023**, *196*, 107040. [CrossRef]
192. Hua, Y.; Lisak, G.; Zhang, Z. Deep Eutectic Solvent for Green Recycling of Spent Lithium-Ion Batteries: A Review of Progress and Challenges. *Sep. Purif. Technol.* **2025**, *378*, 134576. [CrossRef]
193. Kityk, A.; Pavlik, V.; Hnatko, M. Reshaping the Future of Battery Waste: Deep Eutectic Solvents in Li-Ion Battery Recycling. *J. Energy Storage* **2024**, *97*, 112990. [CrossRef]
194. Tang, L.; Ru, J.; Cheng, M.; Zhou, Z.; Hua, Y.; Wang, D. Enhanced Leaching Capacity and Industrial Scale for Critical Metals Recovery from Spent Lithium-Ion Batteries via H2O-Temperature Regulation Method. *Energy Storage Mater.* **2026**, *86*, 104971. [CrossRef]
195. Mukherjee, A.; Apte, S.; Turkane, S.D. Deep Eutectic Solvents and Electrochemical Metal Recycling: A Comprehensive Method Review. *Results Chem.* **2026**, *27*, 103455. [CrossRef]
196. Cui, R.; Ran, Y.; Shu, D.; Huang, Q.; Song, Q.; Wang, H.; Zhu, J.; Yuan, W. Recent Advances in Green Deep Eutectic Solvents for Lithium-Ion Battery Recycling: A Perspective on Bibliometric Analysis. *J. Environ. Manag.* **2025**, *377*, 124670. [CrossRef]
197. Moganti, L.K.; Dutta, D. Deep Eutectic Solvents in E-Waste Recycling: Preparation, Properties, and Hydrometallurgical Metal Recovery. *RSC Adv.* **2026**, *16*, 5228–5251. [CrossRef]
198. Mani, K.A.; Kumar, L.; Barrios, N.; Agate, S.; Mittal, A.; Yarbrough, J.; Jameel, H.; Lucia, L.; Pal, L. Emergence of Deep Eutectic Solvents (DES): Chemistry, Preparation, Properties, and Applications in Biorefineries and Critical Materials. *Prog. Mater. Sci.* **2026**, *157*, 101586. [CrossRef]
199. Sanjeeta; Singh, A.; Kavirajwar, J. Dynamic Properties and Diverse Applications of Deep Eutectic Solvents. *J. Ion. Liq.* **2025**, *5*, 100135. [CrossRef]
200. Martínez, G.M.; Townley, G.G.; Martínez-Espinosa, R.M. Controversy on the Toxic Nature of Deep Eutectic Solvents and Their Potential Contribution to Environmental Pollution. *Heliyon* **2022**, *8*, e12567. [CrossRef]
201. Zhu, A.; Bian, X.; Han, W.; Wen, Y.; Ye, K.; Wang, G.; Yan, J.; Cao, D.; Zhu, K.; Wang, S. Microwave-Ultra-Fast Recovery of Valuable Metals from Spent Lithium-Ion Batteries by Deep Eutectic Solvents. *Waste Manag.* **2023**, *156*, 139–147. [CrossRef]
202. Mannu, A.; Di Pietro, M.E.; Basilico, M.Y.; Bontempi, E.; Mele, A. Assessing the Sustainability of Solvometallurgy for Black Mass Processing—The LEACH (Low-Impact Extraction and Assessment of CHemical Solvometallurgy) Tool. *Green Chem.* **2026**, *28*, 5210–5225. [CrossRef]

Disclaimer/Publisher's Note: The statements, opinions and data contained in all publications are solely those of the individual author(s) and contributor(s) and not of MDPI and/or the editor(s). MDPI and/or the editor(s) disclaim responsibility for any injury to people or property resulting from any ideas, methods, instructions or products referred to in the content.